Provided for non-commercial research and education use.
Not for reproduction, distribution or commercial use.

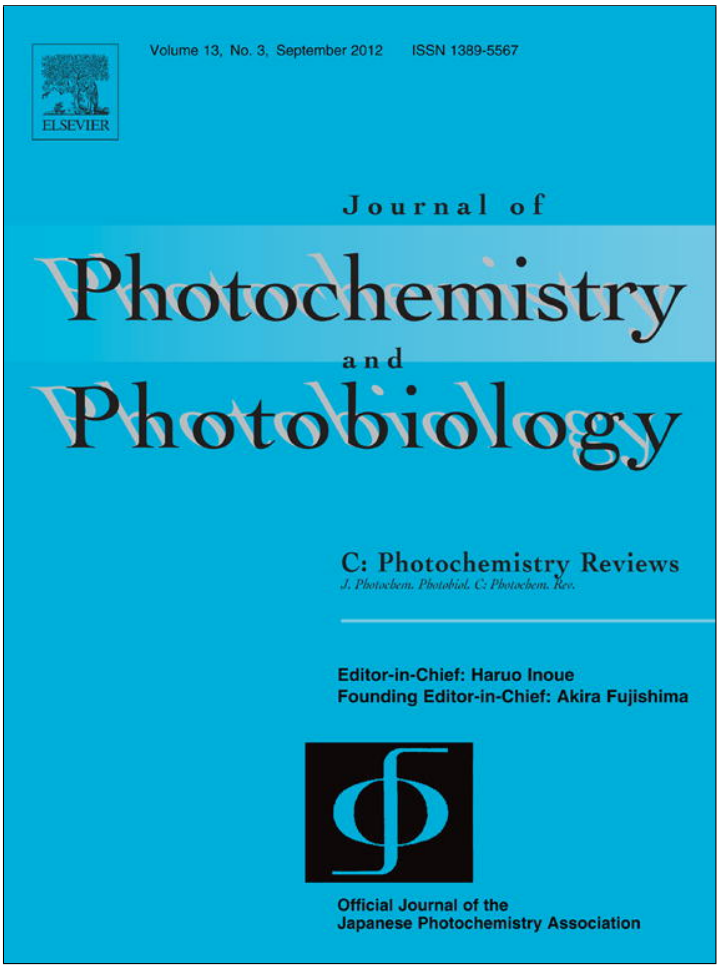

This article appeared in a journal published by Elsevier. The attached copy is furnished to the author for internal non-commercial research and education use, including for instruction at the authors institution and sharing with colleagues.

Other uses, including reproduction and distribution, or selling or licensing copies, or posting to personal, institutional or third party websites are prohibited.

In most cases authors are permitted to post their version of the article (e.g. in Word or Tex form) to their personal website or institutional repository. Authors requiring further information regarding Elsevier's archiving and manuscript policies are encouraged to visit:

http://www.elsevier.com/copyright

Author's personal copy

Journal of Photochemistry and Photobiology C: Photochemistry Reviews 13 (2012) 224–245

Contents lists available at SciVerse ScienceDirect

Journal of Photochemistry and Photobiology C: Photochemistry Reviews

journal homepage: www.elsevier.com/locate/jphotochemrev

Review

Overview on oxidation mechanisms of organic compounds by TiO_2 in heterogeneous photocatalysis

Vincenzo Augugliaro[a], Marianna Bellardita[a], Vittorio Loddo[a], Giovanni Palmisano[a,*], Leonardo Palmisano[a], Sedat Yurdakal[b]

[a] "Schiavello-Grillone" Photocatalysis Group – Dipartimento di Ingegneria Elettrica, Elettronica e delle Telecomunicazioni, di tecnologie Chimiche, Automatica e modelli Matematici – Università degli Studi di Palermo, Viale delle Scienze (Ed. 6) – 90128 Palermo, Italy

[b] Kimya Bölümü, Fen-Edebiyat Fakültesi, Afyon Kocatepe Üniversitesi, Ahmet Necdet Sezer Kampüsü, 03100, Afyon, Turkey

ARTICLE INFO

Article history:
Received 7 February 2012
Received in revised form 23 March 2012
Accepted 13 April 2012
Available online 25 April 2012

Keywords:
Photocatalysis
Reaction mechanisms
Organic reactions
TiO_2

ABSTRACT

This review provides the reader with a general overview on heterogeneous photocatalytic oxidation mechanisms in the presence of TiO_2, with a special address to conversion of aliphatic and aromatic organic species. The aim was to clarify the steps of the photo-oxidation of the various classes of compounds and to relate them with the properties of the catalysts and the experimental conditions used. Reactions carried out to perform complete degradation and photocatalytic partial oxidations have been deeply discussed. Recent isotopic studies highlighted new reaction pathways concerning partial oxidation of alcohols to aldehyde and oxidation of benzene while EPR investigations confirmed that not only the photogenerated hole but also the OH radicals are involved in the oxidation of the substrates.

© 2012 Elsevier B.V. All rights reserved.

Contents

1. Introduction 225
2. Aliphatic oxidation 225
3. Aromatic oxidation 231
4. Conclusions 235
References 235

Vincenzo Augugliaro (1949) received the doctor degree in chemical engineering from the University of Palermo (Italy) in 1975 cum laude. He is full professor of transport phenomena at the Faculty of Engineering of the University of Palermo. Vincenzo Augugliaro has contributed to the following fields: chemical absorption kinetics, biochemical reactor modelling, diffusional kinetics in metalliding alloys, chemical kinetics of heterogeneous photocatalytic systems, modelling of heterogeneous photoreactors, radiation field modelling in absorbing-reacting media, advanced oxidation processes for environment remediation.

Marianna Bellardita (1975) graduated in Palermo in 2004 in chemical engineering and got a PhD in chemical and new materials technologies in 2008 and she is currently post-doc fellow at the University of Palermo. Her research activity deals with the preparation and characterization of photocatalysts, both in the form of powders and in the form of film, mainly for the degradation of pollutants and she is co-author of many papers and communications in international conferences on these topics. During her philosophical doctorate she worked at the preparation of catalysts supported on silica, metacaolino and clinker for integration in self-cleaning materials in a project with the Italcementi Group.

* Corresponding author.
E-mail address: giovanni.palmisano@unipa.it (G. Palmisano).

1389-5567/$20.00 © 2012 Elsevier B.V. All rights reserved.
http://dx.doi.org/10.1016/j.jphotochemrev.2012.04.003

Author's personal copy

Vittorio Loddo (1963) obtained the degree in chemical engineering in 1993 and he is presently researcher at the Department of Chemical Engineering. He is assistant professor of transport phenomena and his research work is presently carried out in the field of reactor modelling for photocatalytic reactions, radiation field modelling in absorbing–reacting media, advanced oxidation processes for environment remediation and he is author of many publication in international journal and books.

Giovanni Palmisano (1981) graduated in chemical engineering in 2005 and got his PhD in chemical and materials engineering in 2009. Since then he has continuously worked in basic and applied research at Universities of Palermo, Roma Tor Vergata, Calabria, at CNR in Palermo and at CSIC in Madrid. Main research activities have been carried out in photocatalytic process, with a special attention to photo-reactors and also preparation and characterization of materials for catalysis and 3rd generation photovoltaics.

Leonardo Palmisano (1950), received the doctor degree in chemistry from the University of Palermo (Italy) in 1973 cum laude. He is full professor of chemistry at University of Palermo. His main field of interest is heterogeneous photocatalysis and he is author of many papers and communications in international conferences. He has been invited as visiting researcher (Bradford University, Bradford, UK) or visiting professor (Hokkaido University, Sapporo, Japan) or as lecturer in many universities all over the world. Moreover, he is co-author of a didactic book Fondamenti di Chimica published in Italy by Edises, and in Spain by Ariel Ciencia.

Sedat Yurdakal (1977) received his high degree in chemistry in 2000 at the University of Anadolu, Eskişehir, Turkey. He started to work as a research assistant at the University of Afyon Kocatepe in 2001. He performed his PhD Thesis work at the University of Palermo and University of Anadolu from 2003 to 2010. Now, he is working as assistant professor at the University of Afyon Kocatepe. He has published several papers in international journals and books on selective photocatalytic oxidations in water, remediation of harmful compounds and preparation of new materials containing TiO_2.

1. Introduction

Heterogeneous photocatalysis has been a broadly studied field in the last decades, in which the main applications analyzed were those correlated to the use of light and a solid catalyst, irradiated by light with an appropriate wavelength, in order to degrade liquid and gas-phase pollutants [1]. Unselective degradation takes place by means of parallel and series redox reactions where the compounds oxidized are the target ones, while the oxidizing reagent is most commonly molecular oxygen in its radical forms or holes (h^+) formed upon irradiation on catalyst sites.

Many semiconductors have been used as photocatalysts: TiO_2, ZnO, WO_3, CdS and NiO can be found among the best performing ones. Each photocatalyst is characterized by a different band gap energy and oxidizing power.

TiO_2 semiconductor is activated by a mechanism involving radical reactive species, through the following series reactions:

$$TiO_2 + h\nu \rightarrow TiO_2(e^-_{(CB)} + h^+_{(VB)}) \quad (1)$$

$$OH^- + h^+_{(VB)} \rightarrow {}^{\bullet}OH \quad (2)$$

$$O_2 + e^-_{(CB)} \rightarrow {}^{\bullet}O_2^- \quad (3)$$

$${}^{\bullet}O_2^- + H^+ \rightarrow {}^{\bullet}HO_2 \quad (4)$$

$$2{}^{\bullet}HO_2 \rightarrow O_2 + H_2O_2 \quad (5)$$

$$H_2O_2 + {}^{\bullet}O_2^- \rightarrow OH^- + {}^{\bullet}OH + O_2 \quad (6)$$

The radical species resulting the most active in carrying out oxidation were often found to be ${}^{\bullet}O_2{}^-$, ${}^{\bullet}HO_2$ and ${}^{\bullet}OH$. The possibility to employ photocatalytic reactions in order not only to perform complete oxidation but also to give rise to partial oxidation with the aim of providing an alternative to more conventional synthetic pathways has attracted a growing interest of many researchers [2]. Many case studies on different substrates have been fully developed hence demonstrating that this opportunity is real. Significant examples of photocatalytic processes employed for synthetic purposes have been produced, showing that the use of solar light as a reagent in oxidative catalysis can be particularly relevant to realize innovative and economically consistent processes and, at the same time, to move toward a sustainable chemistry that has a minimal environmental impact.

On one contrary, the application of photocatalytic reactions to water and air remediation has been widely studied. In particular TiO_2 presents a precious property that is the unselectivity in oxidation reactions. Very few compounds are known that cannot be degraded by TiO_2 irradiated by UV-light [3].

2. Aliphatic oxidation

In this section some case studies on photocatalytic oxidation of aliphatic species [4,5] will be discussed. Oxygenation of alkanes, for example, is a reaction of particular interest in both partial oxidation and air remediation fields [6–8].

Oxidation is thought to be initiated via reaction 7a or 7b, after activation of a photocatalyst:

$$RCH_3 + h^+ \rightarrow {}^{\bullet}RCH_2 + H^+ \quad (7a)$$

$$RCH_3 + {}^{\bullet}OH \rightarrow {}^{\bullet}RCH_2 + H_2O \quad (7b)$$

The alkyl radical can react as showed in reaction 8 or alternatively via series reactions (9a)–(9d):

$${}^{\bullet}RCH_2 + {}^{\bullet}OH \rightarrow RCH_2OH \quad (8)$$

$${}^{\bullet}RCH_2 + O_2 \rightarrow RCH_2OO^{\bullet} \quad (9a)$$

$$RCH_2OO^{\bullet} + RCH_3 + RCH_2OOH + {}^{\bullet}RCH_2 \quad (9b)$$

$$RCH_2OOH + e^- \rightarrow RCH_2O^{\bullet} + {}^-OH \quad (9c)$$

$$RCH_2O^{\bullet} + RCH_3 \rightarrow RCH_2OH + {}^{\bullet}RCH_2 \quad (9d)$$

The obtained alcohol RCH_2OH can be further oxidized to the corresponding aldehyde and acid by the following series reactions:

$$RCH_2OH + {}^{\bullet}OH \rightarrow RCH_2O^{\bullet} + H_2O \quad (10a)$$

$$RCH_2O^{\bullet} + {}^{\bullet}OH \rightarrow RCHO + H_2O \quad (10b)$$

$$RCHO + {}^{\bullet}OH \rightarrow R{}^{\bullet}COOH \quad (10c)$$

$$R{}^{\bullet}CHOOH + {}^{\bullet}OH \rightarrow RCOOH + H_2O \quad (10d)$$

Ketones can be obtained starting from secondary alcohols by the following series reactions:

$$RCHOHR' + {}^{\bullet}OH \rightarrow R{}^{\bullet}CHOR' + H_2O \quad (10e)$$

$$R{}^{\bullet}CHOR' + {}^{\bullet}OH \rightarrow RCOR' + H_2O \quad (10f)$$

By considering for instance the simplest hydrocarbon, methane, mainly obtained by natural gas, which is copiously present in nature, low-yield photocatalytic oxidation has been achieved mainly by using near-UV irradiated semiconductors such as TiO_2, WO_3, NiO and Ga_2O_3 [9–15].

Author's personal copy

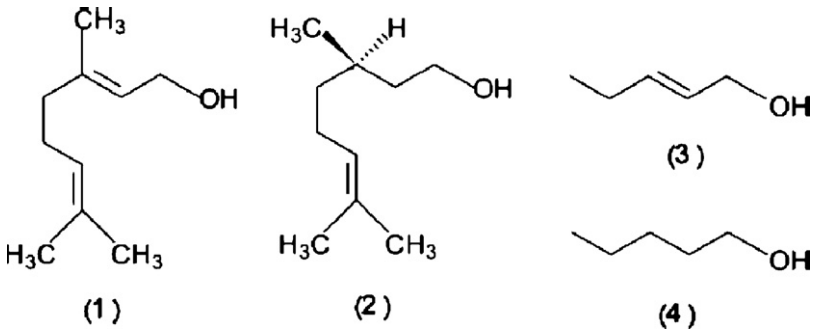

Fig. 1. Allylic alcohols photocatalytically oxidized [16].

Industrially natural gas is converted to synthesis gas (a mixture of CO and H_2), formed through a process known as steam reforming, carried out under high temperature (973–1373 K). Methanol is further obtained by synthesis gas, in its turn used to synthesize highly-requested compounds as formaldehyde, acetic acid and MTBE (methyl tertiary-butyl ether). Yet methanol is employed as a fuel source in fuel cells.

Under visible light irradiation the methane conversion to methanol, hydrogen and acetic acid in the presence of La-doped WO_3 and of an electron transfer molecule in aqueous suspensions (at ca. 367 K) is thought to proceed as reported in the following:

$$La/WO_3 \xrightarrow{h\nu,\ \lambda>410\,nm} e^-_{CB} + h^+_{VB} \quad (11a)$$

$$e^-_{CB} + MV^{2+} \rightarrow MV^{\bullet+} \quad (11b)$$

$$h^+_{VB} + H_2O \rightarrow H^+ + {}^{\bullet}OH \quad (11c)$$

$$MV^{\bullet+} + H^+ \rightarrow \tfrac{1}{2}H_2 + MV^{2+} \quad (11d)$$

$$CH_4 + {}^{\bullet}OH \rightarrow CH_3{}^{\bullet} + H_2O \quad (11e)$$

$$CH_3{}^{\bullet} + H_2O \rightarrow CH_3OH + \tfrac{1}{2}H_2 \quad (11f)$$

where MV stands for methyl viologen. Conversion of methane is low (ca. 4% and 10% in the presence of hydrogen peroxide) and no reaction is observed at room temperature. A significant enhancement of the process was reached by using methane hydrates, now obtaining significant conversions even at very low temperatures (268 K). Methane hydrates form in the ocean at depths between ca. 280 and 4000 m enabling higher concentrations of methane in water, higher even than those obtained in water-methane pressurized systems. Hence the produced methanol in this case was more than 4-fold than that of methane–water system. The author also observed that irradiating the suspensions with UV–vis rather than visible light lowered the quantity of alcohol, causing an overoxidation of methanol.

The oxidation of aliphatic alcohols by TiO_2 has been studied in various media. Molinari et al. [16] have investigated also the photocatalytic partial oxidation of some allylic alcohols (showed in Fig. 1) as geraniol (1) and trans-2-penten-1-ol (3) along with primary alcohols as citronellol (2) and 1-pentanol (4).

The study of the reaction mechanism by EPR revealed that not only the photogenerated hole but also the OH radical are involved in the oxidation of the substrate. In the absence of water the photocatalytic partial oxidation of geraniol produces only citral; however, in the presence of water, OH radical can attack geraniol not selectively giving rise to the total and not selective degradation of the substrate. Moreover the authors indicate that the presence of water inhibits the adsorption of geraniol and so it has a negative effect on the formation of citral abating the selectivity. Already a 2% of water increases significantly the polarity of the medium thus decreasing the adsorption of the substrate that competes with water for the adsorption sites.

As far as the two primary alcohols (geraniol and citronellol) are concerned, their great hydrophobic tails hinder the adsorption of these molecules in the presence of water that displaces easily these substrates from the surface of the photocatalyst. On the contrary, 1-pentanol and trans-2-penten-1-ol are less influenced by the presence of water; consequently they are able to interact with the surface of the photocatalyst even when the surface is partially polar. Short alcohols as methanol and 2-propanol [17,18] are degraded even in a water medium.

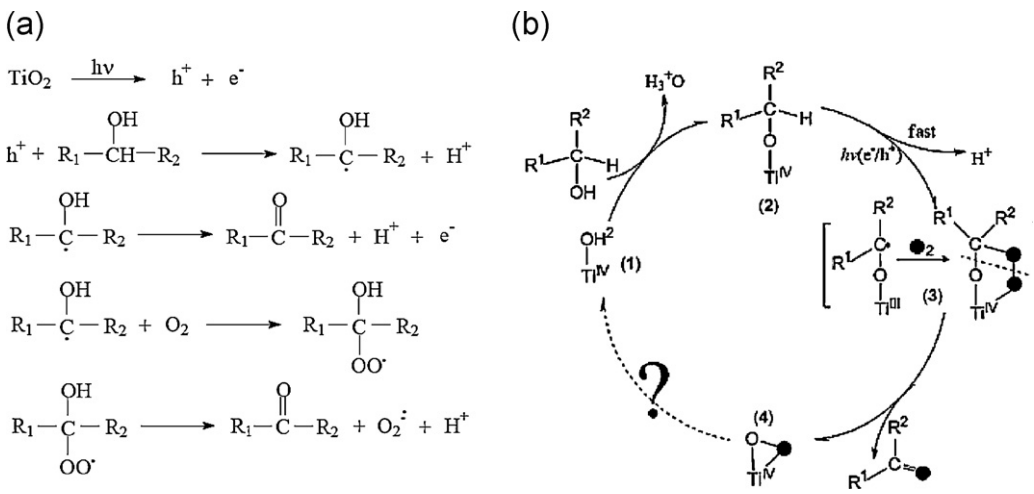

Fig. 2. (a) Reaction scheme of photocatalytic alcohol oxidation in water [16] and (b) in benzotrifluoride [20].

Author's personal copy

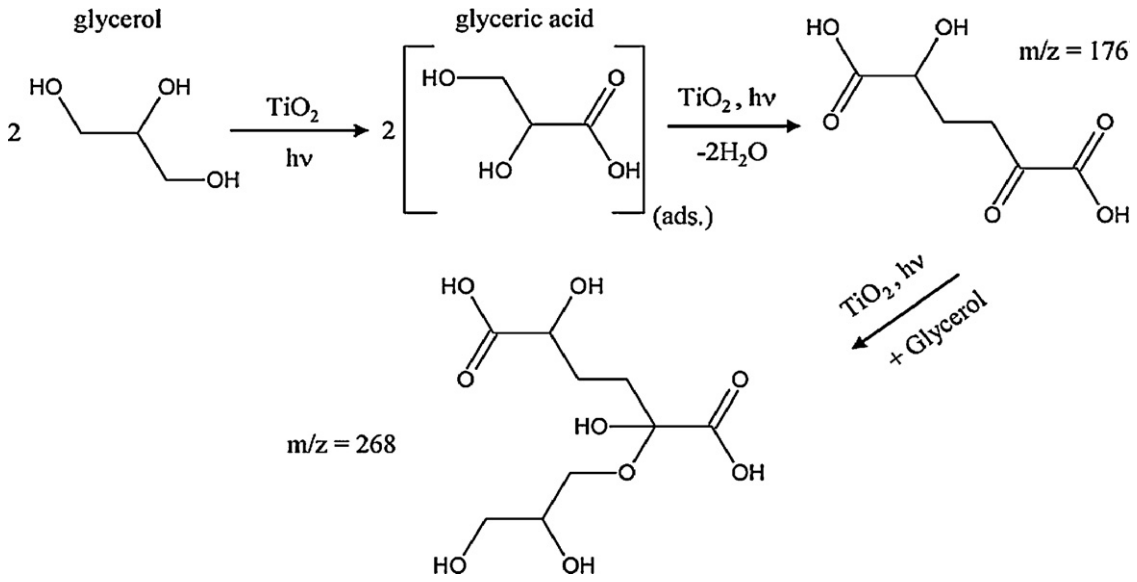

Fig. 3. Photocatalytic oxidation mechanism of glycerol [21].

Fig. 2 shows the hypothesized oxidation mechanisms for alcohols in water (Fig. 2a) and in an organic solvent (Fig. 2b) [19,20]. Zhang et al. [19,20] studied the mechanism of the photocatalytically oxidative transformation of alcohols performed in benzotrifluoride (BTF) by using bare TiO_2 anatase. They found an oxygen transfer from molecular O_2 to the alcohol. The oxygen atom of the alcohol is completely replaced by one of the oxygen atoms of the dioxygen molecule, i.e. the process occurs by the selective cleavage of the C—OH bond with the concomitant formation of a C=O bond to obtain the final product, where O comes from O_2. The mechanism proposed by authors (Fig. 2b) is the following one. The alcohol molecule is adsorbed onto the surface of TiO_2 by a deprotonation process, hence it reacts with the photogenerated hole on the TiO_2 surface forming a carbon radical whereas the electron transforms Ti(IV) in Ti(III). Both carbon radical and Ti(III) easily react with O_2 and a Ti peroxide intermediate is formed. The cleavage of this species gives rise to carbonylic species, coming from the partial oxidation of the alcohol. The same authors carried out the same reaction in the presence of Brönsted acids and they observed an enhancement of both reaction rate and selectivity. The effect is related to the decomposition of the relatively stable side-on peroxide intermediate by the protons of the Brönsted acids, which can clean the catalytic Ti-OH_2 sites. This finding opens a new path to obtain high selectivity and conversion by TiO_2 photocatalysis.

Among aliphatic alcohols, glycerol (1,2,3-propanetriol) has widespread applications; this molecule is indeed used in toothpastes, pharmaceuticals, cosmetics, soaps and as sweetener in cakes and wetting agent in tobacco. Glycerol is also a co-product of oils and fats industries and hence available in huge amounts. Moreover, nowadays glycerol is also obtained from biodiesel: one

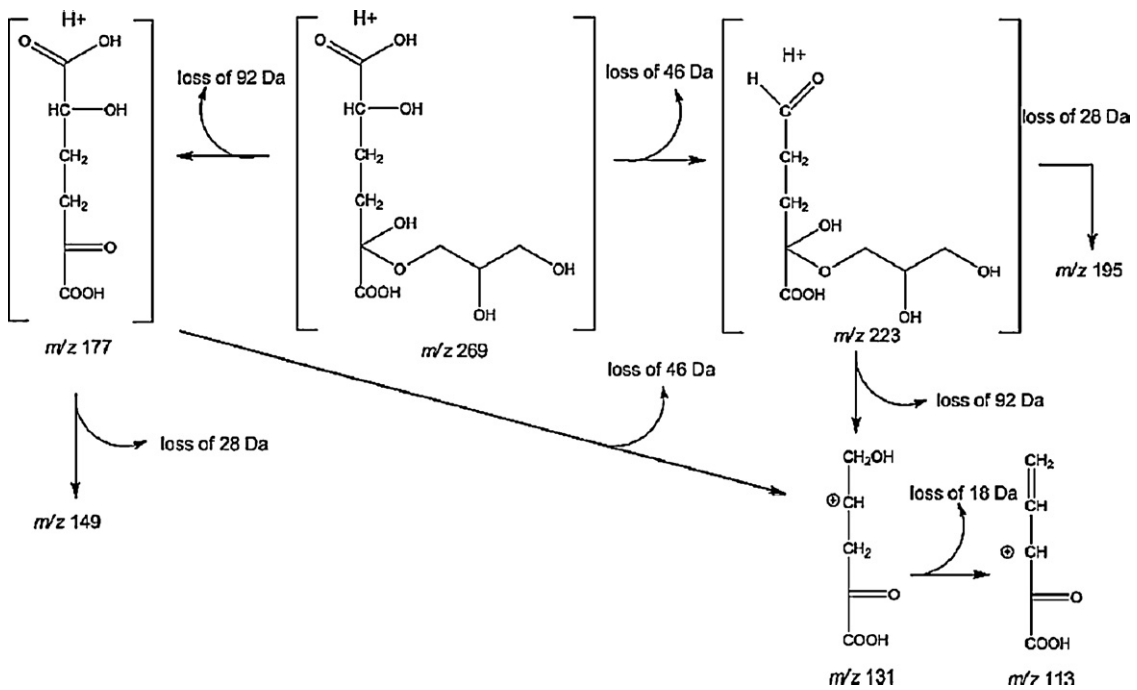

Fig. 4. Oxidated species from glycerol detected by means of ESI-MS [21].

Author's personal copy

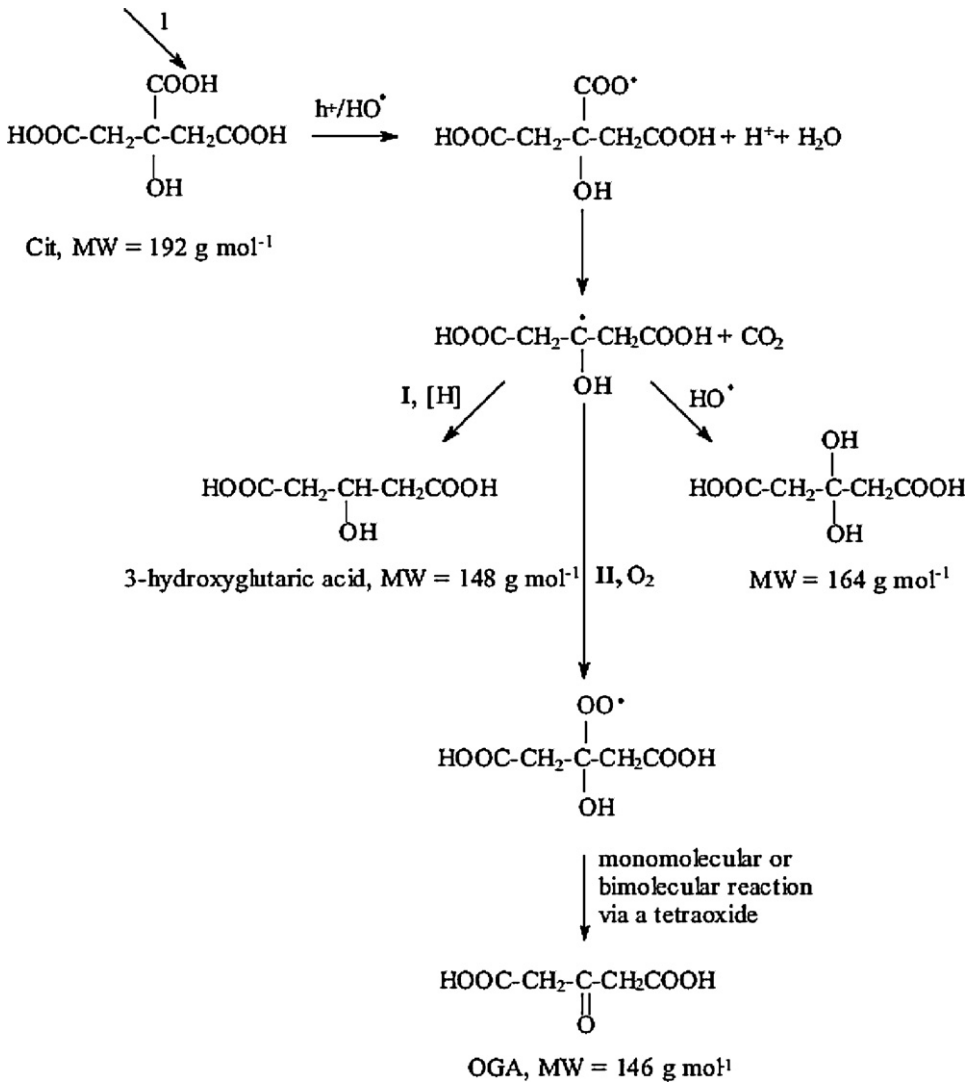

Fig. 5. Reaction scheme of photocatalytic oxidation of citric acid upon attack on position (1) [26].

ton of biodiesel produces in fact about 100 kg of pure glycerol. Few amounts of glycerol, with respect of its high accessibility, are used in synthesis of polyethers and esters. Many products can be obtained from its partial oxidation: 1,3-dihydroxyacetone (DHA), glyceraldehyde (GAD), glyceric acid, glycolic acid, hydroxypyruvic acid, mesoxalic acid, oxalic acid, tartronic acid and all of them are considered chemicals for highly specialized applications. Photocatalytic oxidation of glycerol [21–25] has been reported to occur in water suspensions of TiO_2 photocatalyst through two parallel pathways: one leading to the direct mineralization to CO_2 via a series of adsorbed and not detectable intermediates; the other one producing various oxidized species (reported in Figs. 3 and 4). Production of CO_2 results clear from the data recorded by a TOC analyzer, showing a decrease of organic carbon since the beginning of the reaction. On the other side ESI-MS analyses demonstrated the formation of 1,3-dihydroxyacetone and glyceraldehyde as peaks at m/z 145. Sequential enrichment of the solution with these two species allowed to assign the peak at m/z 145 to [DHA + MeOH + Na^+] and [GAD + MeOH + Na^+] adducts.

Organic acids [26–30] can also be oxidized by heterogeneous photocatalysis. Decarboxylation typically occurs finally bringing to mineralization with the formation of CO_2 and H_2O. The degradation pathways for citric acid by TiO_2 were studied in a water suspension contained in a batch reactor or in a recirculating reactor, by analyzing its degradation intermediate products [26]. In particular the most abundant product formed was 3-oxoglutaric acid (OGA), but several other compounds, like acetoacetic, lactic, pyruvic, malic, glyoxylic, acetic and formic acids plus acetone were found.

Oxidation attack on citric acid is possible on different point of the molecule: (1) on the carboxyl group bound to the tertiary carbon, (2) on the methylenic groups, (3) on the OH bound to the central carbon, or (4) on the carboxyl groups bound to the methylenic groups. Several routes can give rise to the formation of the main intermediate found, i.e. OGA.

Fig. 5 shows the three hypothesized reaction routes for the first steps of citric acid oxidation, upon attack on position (1): hole or hydroxyl radical attack gives rise to a radical, which can decay by the three routes. From left to right, 3-hydroxyglutaric acid, OGA and the hydrate form of OGA are formed. The pattern of intermediates concentrations suggests that the initial reaction mechanism follows that shown in Fig. 5, with subsequent thermal decomposition of OGA to acetoacetic acid (AAA) and acetone, as reported in literature [26]. Photocatalytic oxidation of acetoacetic acid is, indeed, inhibited in the presence of OGA.

Oxidation attack on methylenic groups (position (2)) gives rise to H-abstraction to the α-hydrogen leading to products indicated in Fig. 6 through routes II and III. Although these routes are less

Author's personal copy

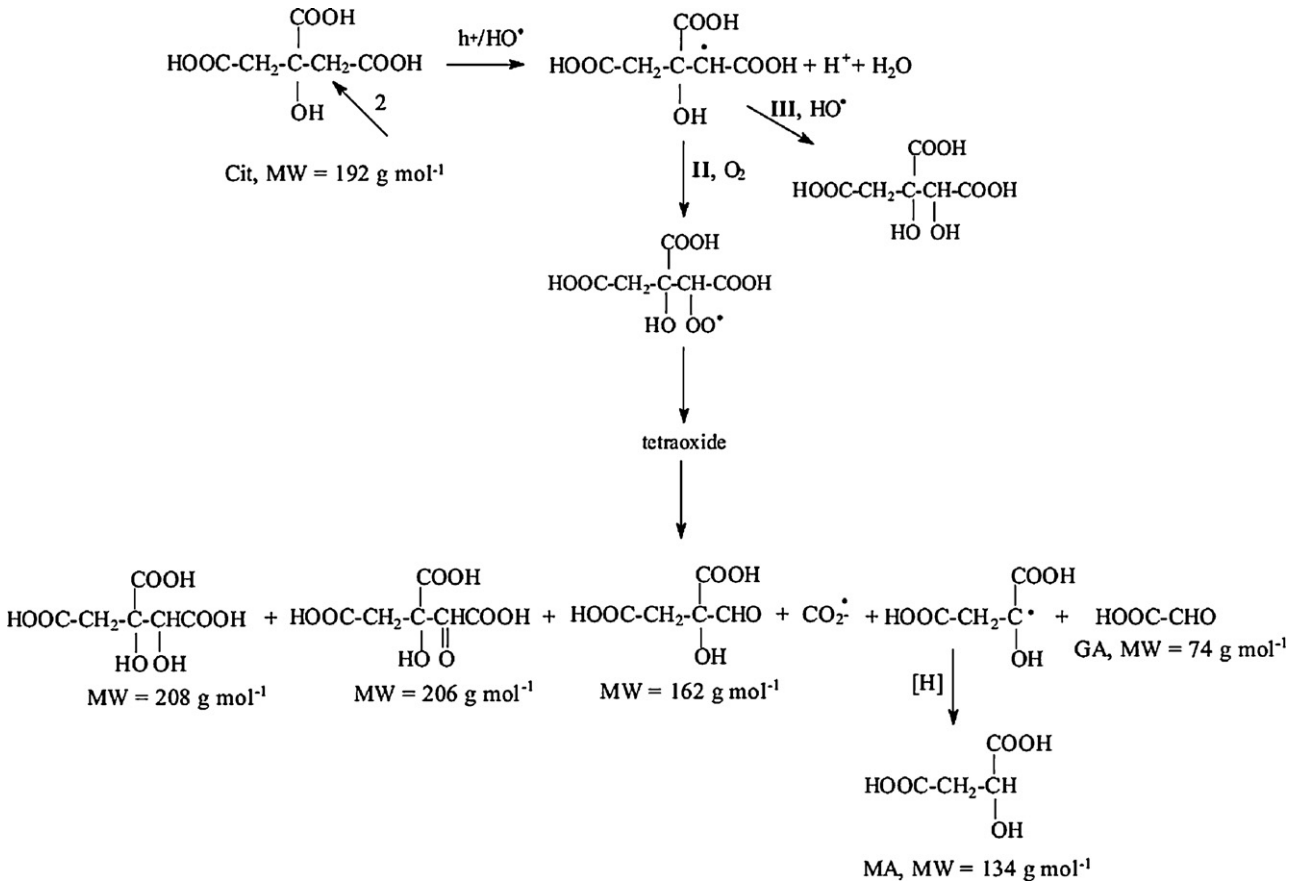

Fig. 6. Reaction scheme of photocatalytic oxidation of citric acid upon attack on position (2) [26].

probable, [27] they become significant at high hydroxyl radical concentrations [28].

The attack on position (3), giving rise to an oxyl radical that can be oxidized also to OGA plus •COOH ($CO_2^{\bullet-} + H^+$), was not corroborated by experimental results (Fig. 7). On the other side, attack to position (4) follows similar mechanisms to those analyzed through routes I, II and III (Fig. 8), leading to a carboxyl radical, then to a methylenic radical by decarboxylation, ending in citramalic acid by route I. Citramalic acid, if formed, can react by different routes, ending in acetoacetic acid, among other products. By route II, the peroxyl radical molecule would lead to the alcohol and aldehyde of MW = 164 and 162 g mol^{-1}, respectively. The same alcohol can be formed by route III.

Attack on position (4) has been demonstrated by some analytical evidence [26].

3-Oxoglutaric acid, the main oxidation product of citric acid, can be oxidized both by holes and hydroxyl radicals (free or trapped at the TiO_2 surface) [31]. Oxidation can be carried out to two different points of attack: the carboxyl group (position 1) or the α-hydrogen (position 2). Firstly, the attack could lead to AAA (Fig. 9, route **I**). By route **II**, an alcohol (MW = 118 g mol^{-1}) and an aldehyde (MW = 116 g mol^{-1}) can be formed. These last compounds can be oxidized to oxalacetic acid (MW = 132 g mol^{-1}), that is an unstable β-ketoacid, easily decarboxylated by a thermal reaction probably by a simultaneous photo-Kolbe process like that indicated in Fig. 9.

By attack to α-hydrogen (position 2) of 3-oxoglutaric acid, compounds of MW = 116, 160, 162 g mol^{-1} can form, that generally will be rapidly destroyed or transformed [31] (Fig. 10).

Acetoacetic acid, the main oxidation intermediate of 3-oxoglutaric acid decays only thermally while 3-oxoglutaric acid is present; however, soon after the photocatalytic oxidation becomes effective. Attack can take place in two different positions: the carboxyl group (position 1) or the α-hydrogen (position 2). In the first case (Fig. 11), acetone is produced by route **I**, while route **II** would produce an aldehyde (MW = 72 g mol^{-1}) and an alcohol (MW = 74 g mol^{-1}), both ending in pyruvic acid. Attack on position (2) of AAA (Fig. 12) would lead to products of MW = 116, 118 or 72 g mol^{-1}; this last compound would lead to pyruvic acid.

The photocatalytic degradation of malic acid was studied under ambient conditions in an aqueous TiO_2 suspension [32–34]. Photogenerated holes and hydroxyl radicals are the oxidizing agents. Carbon dioxide evolves soon and a carbon-centered radical is formed:

$$HOOC{-}CH_2{-}CHOH{-}COO^- + h^+ \rightarrow HOOC{-}CH_2{-}^{\bullet}CHOH + CO_2 \quad (12)$$

The corresponding aldehyde is formed upon reaction with molecular oxygen:

$$HOOC{-}CH_2{-}^{\bullet}CHOH + O_2 \rightarrow HOOC{-}CH_2{-}COH + HOO^{\bullet} \quad (13)$$

The decarboxylation of malic acid is a quite rapid process. The initial rapid generation of CO_2 is attributed to this process whereby a significant part of the initial malic acid has been adsorbed and decarboxylated, predominantly forming Intermediate 1 (see Fig. 13) plus traces of other intermediates such as malonic acid. The kinetic data suggest that the malic acid decarboxylation reaction is preferred over subsequent photocatalytic steps in the degradation mechanism. Accordingly carboxylic acids are known to adsorb well onto the TiO_2 surface, particularly at low pH, as the acids are

Author's personal copy

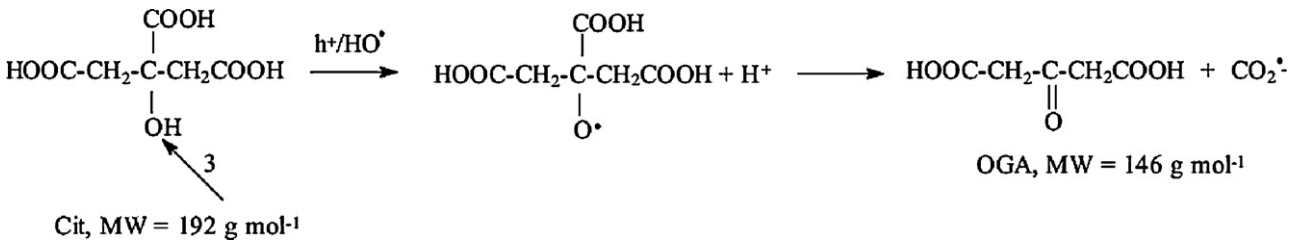

Fig. 7. Reaction scheme of photocatalytic oxidation of citric acid upon attack on position (3) [26].

in their dissociated forms within this pH range and the TiO_2 surface is positively charged [35].

The decline in Intermediate 1 (Fig. 13) represents the beginning of stage II and is characterized by a substantial decrease in the mineralization rate. This indicates that the degradation of Intermediate 1 is less favored than malic acid. It was suggested that the preferential adsorption of malic acid delayed the degradation of this intermediate in the system. The malonic acid concentration also continues to increase. Malonic acid is believed to form by the H atom abstraction and the •OH addition to the aldehyde group

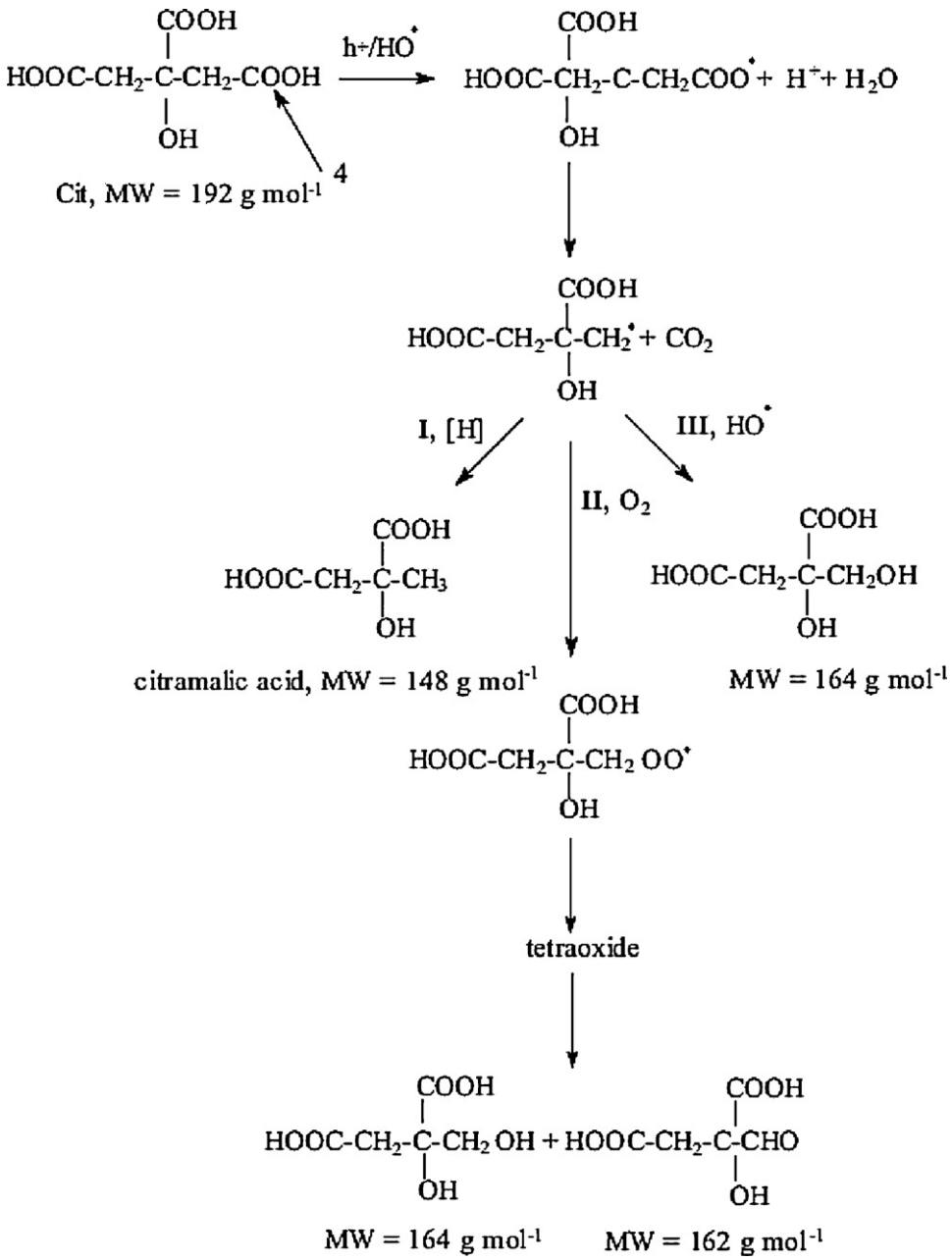

Fig. 8. Reaction scheme of photocatalytic oxidation of citric acid upon attack on position (4) [26].

Author's personal copy

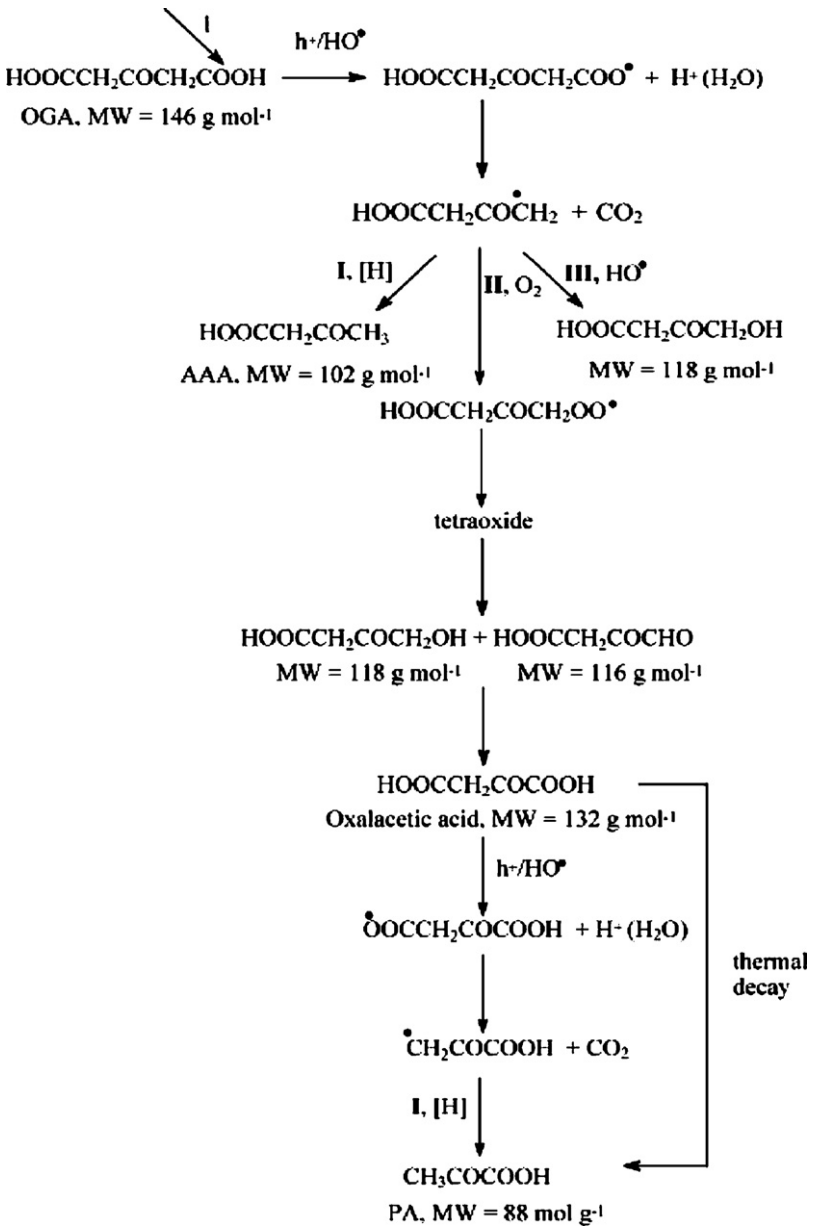

Fig. 9. Reaction scheme of photocatalytic oxidation of 3-oxoglutaric acid upon attack in position (1) [31].

of Intermediate 1. Photodegradation of malonic acid is believed to occur via the photo-Kolbe process, leading to decarboxylation of the C3 chain and creating the acetate radical ($^{\bullet}CH_2COOH$). Further reaction with $^{\bullet}OH$ yields glycolic acid and/or generate acetic acid via the H addition.

Stage III is marked by a decrease in the mineralization rate and encompasses the decrease in acetic acid concentration in the solution. Acetate radical can form oxalic acid by reaction with peroxide radicals as reported by Dolamic and Bürgi [36]; they found oxalic acid to be the major intermediate product during malonic acid mineralization in a small volume flow-through cell. Alternatively, the acetic acid may undergo a sequence of reactions with photogenerated $^{\bullet}OH$ in solution leading to CO_2 formation.

Trichloroethylene oxidation in gas phase has been carried out in a flat-plate photoreactor at inlet concentrations of 100–500 ppm, relative humidities (RH) of 0–62%, gas residence times of 2.5–60.3 s, and incident irradiance of 2.86×10^{-4} meinstein g^{-1} s^{-1} [37–40]. In the first step, trichloroethylene converts to dichloroacetyl chloride ($Cl_2CHCClO$) and in the second one dichloroacetyl chloride converts to phosgene ($COCl_2$), CO_2 and Cl_2 with the aid of one electron–hole pair [37]:

$$CHCl_2CClO + h^+ \rightarrow CHCl_2C^+ClO^{\bullet} \quad (14a)$$

$$e^- + O_2 \rightarrow O_2^{\bullet -} \quad (14b)$$

$$CHCl_2C^+ClO^{\bullet} + O_2^{\bullet -} \rightarrow CHCl_2CCl(O^{\bullet})OO^{\bullet} \quad (14c)$$

$$2CHCl_2CCl(O^{\bullet})OO^{\bullet} \rightarrow 2CHCl_2CCl(O^{\bullet})O^{\bullet} + O_2 \quad \text{Russel mechanism} \quad (14d)$$

$$CHCl_2CCl(O^{\bullet})O^{\bullet} \rightarrow C^{\bullet}HCl_2 + CCl(O^{\bullet})O \quad (14e)$$

$$C^{\bullet}HCl_2 + O_2 \rightarrow C(OO^{\bullet})HCl_2 \quad (14f)$$

$$2C(OO^{\bullet})HCl \rightarrow 2C(O^{\bullet})HCl_2 + O_2 \quad \text{Russel mechanism} \quad (14g)$$

$$C(O^{\bullet})HCl_2 \rightarrow COCl_2 + H^{\bullet} \quad (14h)$$

$$CCl(O^{\bullet})O \rightarrow CO_2 + Cl^{\bullet} \quad (14i)$$

Author's personal copy

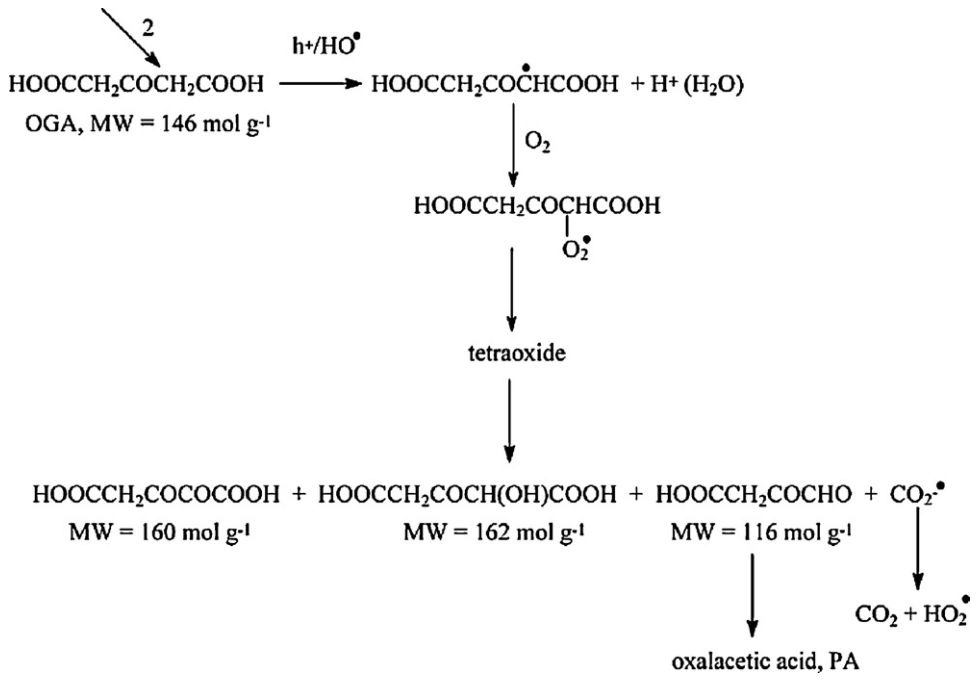

Fig. 10. Reaction scheme of photocatalytic oxidation of 3-oxoglutaric acid upon attack in position (2) [31].

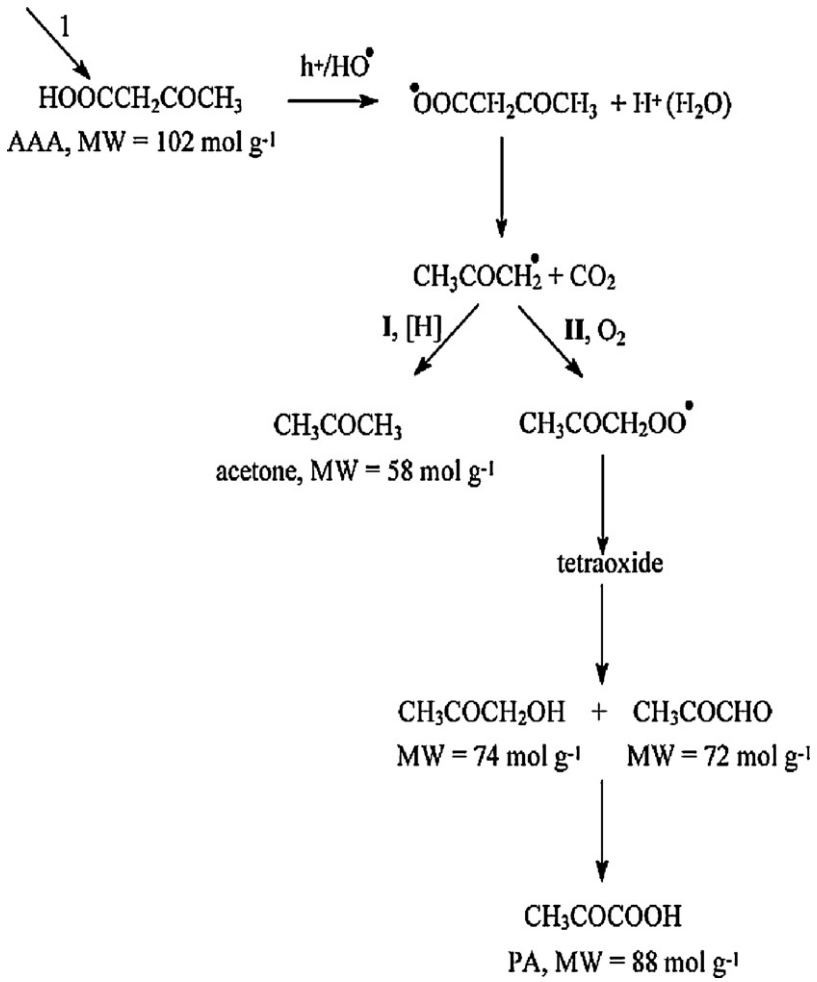

Fig. 11. Reaction scheme of photocatalytic oxidation of acetoacetic acid upon attack in position (1) [31].

Author's personal copy

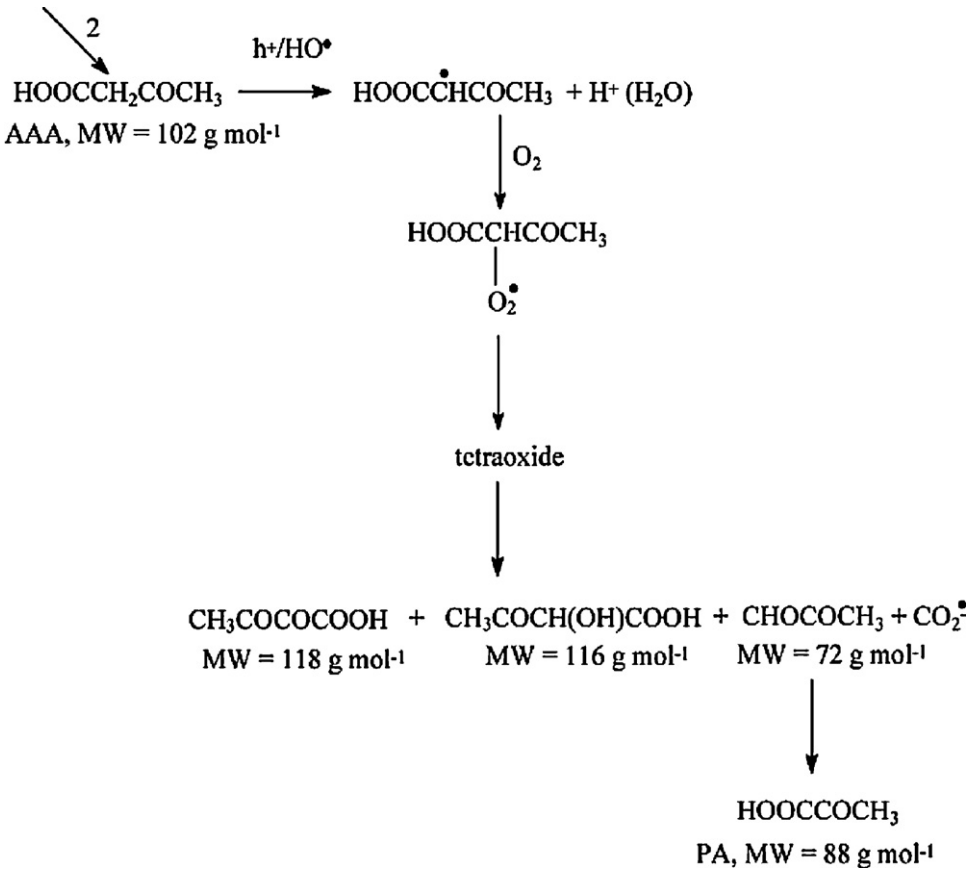

Fig. 12. Reaction scheme of photocatalytic oxidation of acetoacetic acid upon attack in position (2) [31].

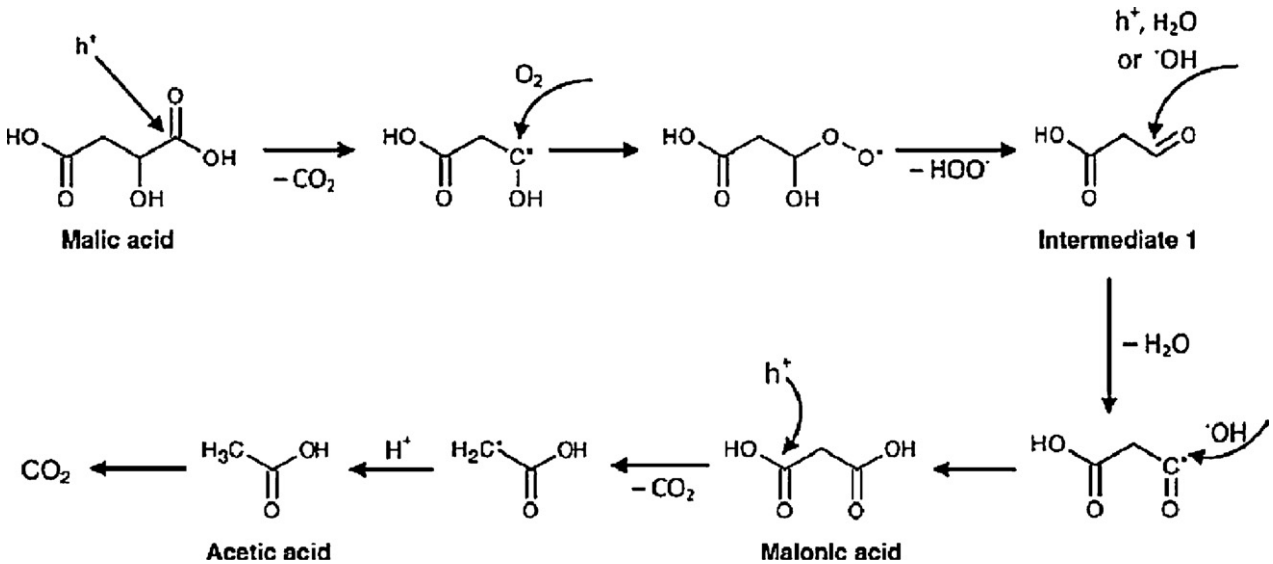

Fig. 13. Reaction scheme of photocatalytic oxidation of malic acid [32].

Author's personal copy

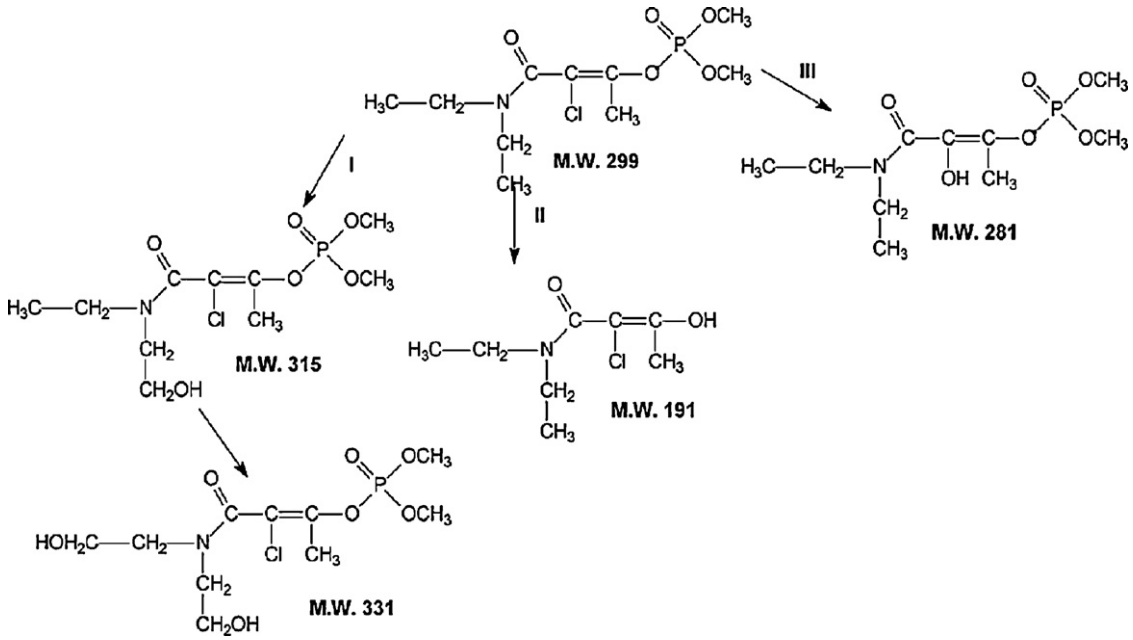

Fig. 14. Transformation pathways of phosphamidon during the photocatalytic degradation over TiO_2 suspensions [46].

Literature reports a mechanism mediated by OH radicals formed by holes attacking adsorbed water, whereas other researchers found the highest photocatalytic degradation rate of trichloroethylene in the absence of water [41]. Two mechanisms, indeed, can be responsible for the inhibitive effect of water: competitive adsorption of water and trichloroethylene on the catalyst surface, and inhibition of an oxidative chain reaction involving the chlorine radical.

In the third step, phosgene is converted to CO_2 and Cl_2, through reaction with one electron–hole pair.

Epoxidation of propene is a reaction of paramount importance in the chemical industry. It has been reported that metal oxide species, when they are highly dispersed on silica, alumina, mesoporous silica or zeolites, exhibit photocatalytic activity for partial oxidation reactions [42]. TiO_2–SiO_2 with low TiO_2 content is active in yielding propylene oxide from propene by molecular oxygen (Fig. 13) at room temperature with a selectivity of 60% [43]. When the highly dispersed active sites are quantum sized isolated metal oxide species, as isolated tethaedra TiO_4 on silica, these species could promote selective oxidations [44]. The excited state is localized at the isolated quantum sized metal oxides, well characterized by their phosphorescence emission [45]. The quantum photocatalysts can induce epoxidation of propene by molecular oxygen

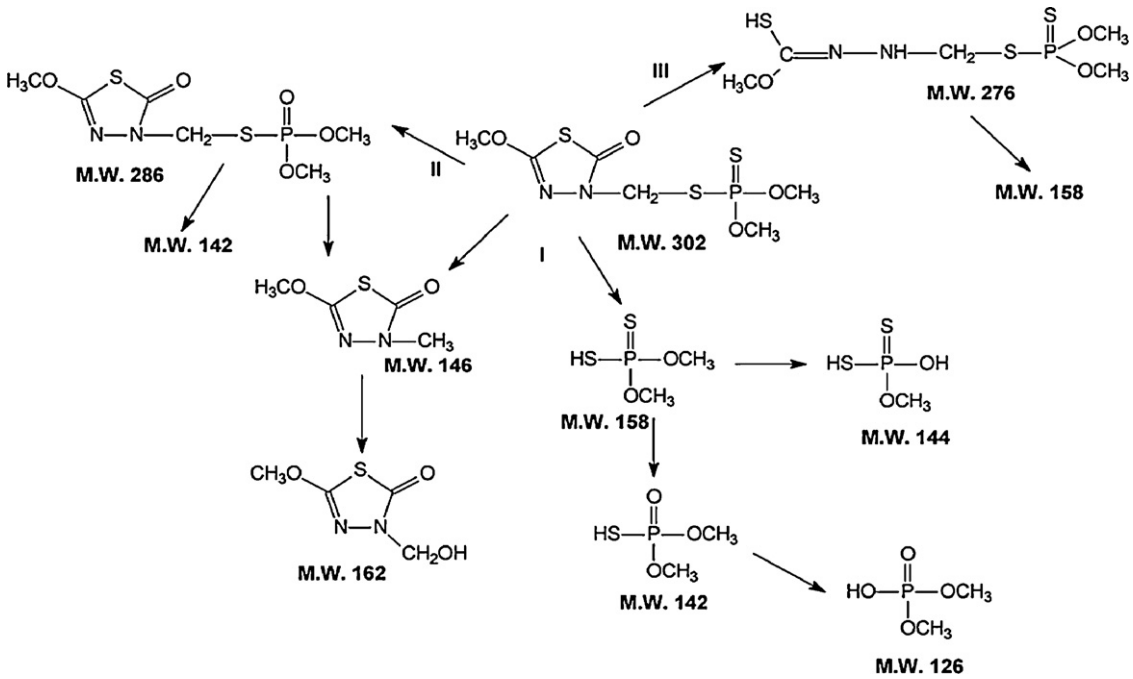

Fig. 15. Transformation pathways of methidathion during the photocatalytic degradation over TiO_2 suspensions [46].

Author's personal copy

but also direct methane coupling or photomethatesis of olefines. Accordingly reaction 15 shows the photocatalytic oxidation of propene over TiO_2-SiO_2 catalysts:

(15)

Organophosphorous pesticides are other relevant aliphatic compounds containing phosphorous and nitrogen atoms, that can be oxidized by applying heterogeneous photocatalysis using TiO_2 [46–50]. This class of compounds constitutes one of the most important groups of insecticides applied in agricultural areas for pest control. The oxidation pathways of azinphos methyl, phosphamidon and methidathion have been, for instance, deeply investigated by using HPLC–MS, ion chromatography and TOC analysis supports.

Analyzing for instance the phosphamidon degradation, four intermediate compounds were detected; they are shown in Fig. 14. The formed molecules are more hydrophilic than the reagent. The predominant transformation pathway is thought to be the one carrying to the intermediate species at $[M+H]^+$ 316. A species at $[M+H]^+$ 332 was also formed and was identified as the bihydroxylated phosphamidon. Two compounds with lower molecular weight were also detected: the first one at $[M+H]^+$ 282 was consistent with the detachment of the chlorine atom, as assessed by the absence in its MS spectrum of the typical chlorine isotopic pattern and was recognized as 2-hydroxy-2-diethylcarbamoyl-1-methylvinyldimethyl phosphate; the second compound at $[M+H]^+$ 192 should be formed through the detachment of the organophosphorus moiety. This hypothesis found support in the contemporaneous formation of phosphate ions.

The cited compounds can be formed through 3 different reaction pathways, summarized in Fig. 14: the first one leads to the formation of the mono and bihydroxylated derivatives. A second pathway leads to the detachment of the organophosphorus moiety, with the formation of the species at $[M+H]^+$ 192 and a third pathway proceeds through the formation of dechlorinated product with $[M+H]^+$ 282.

All the reported intermediates are photocatalytically degraded soon, mineralization being conversely a much slower process.

The photocatalytic degradation pathways of another relevant organophosphorous pesticide, namely methidathion, have been deeply investigated [46]. The formation of the intermediates reported in Fig. 15 involves the breakage of C—S (route I) and P—S (route II) bonds. The former leads to the contemporaneous formation of the species at $[M+H]^+$ 147, 1,3,4-thiadiazol-2(3H)-one,5-methoxy-3-methyl and at $[M+H]^+$ 159, O,O-dimethylhydrogen dithiophosphate. The latter brings about the formation of the species at $[M+H]^+$ 287.

A parallel transformation involves the breakage of the thiadiazolic ring, with the formation of a species at $[M+H]^+$ 277, that still contains three sulfur atom (see pathway III). The elimination of a molecule of CH_3OCH_2SH in its MS/MS spectrum supports the hypothesis of the ring cleavage. Analogously to pathway I, the molecule could then break down with the release of O,O-dimethylhydrogen dithiophosphate.

Further oxidation of intermediates is highlighted in Fig. 15. Complete mineralization of the compound through the formation of ionic species could be obtained. As far as the fate of the nitrogen is concerned, it was released mainly as ammonium ions.

3. Aromatic oxidation

In this section some case studies on photocatalytic oxidation of aromatic species [51–73] will be discussed. Photocatalytic oxidation of benzene was studied in aqueous solutions using different kinds of TiO_2 powders [74–77]. The main intermediate of the reaction was phenol that was subsequently converted into CO_2 via many oxidation steps. It has been proposed that phenol is produced as a result of reaction between benzene and an $HO^\bullet$ radical, which is produced by oxidation of an OH group on TiO_2 by a photogenerated hole. Bui et al. [74], by means of isotopic studies using a stable isotope of oxygen (^{18}O) included in $H_2{}^{18}O$ and $^{18}O_2$, determined two different oxygen sources for the hydroxylation of benzene: water and molecular oxygen (Fig. 16). The processes using water and molecular oxygen as the oxygen sources are ascribed,

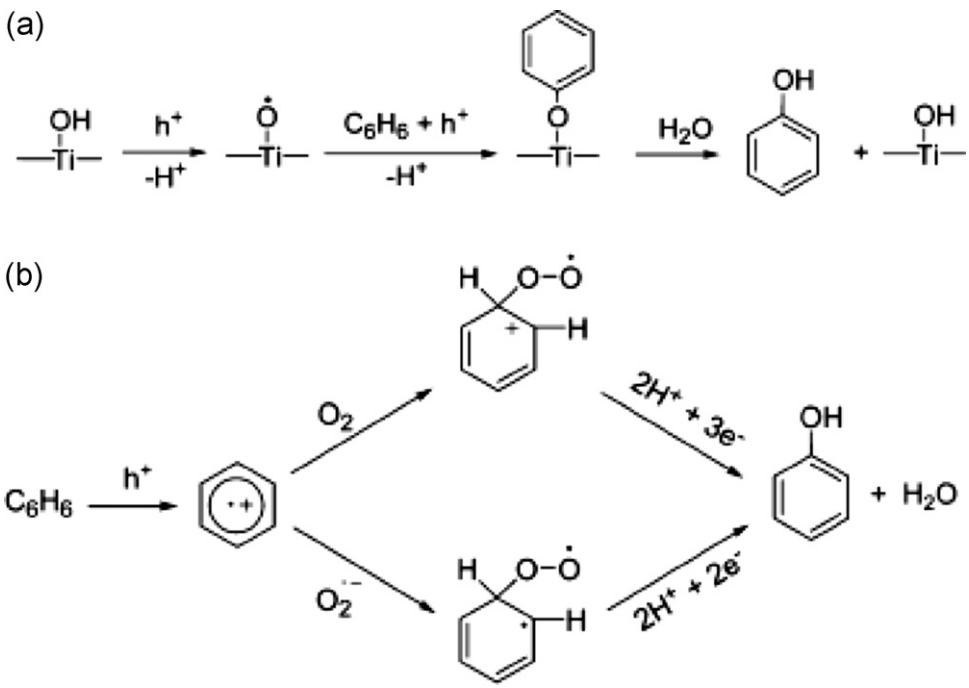

Fig. 16. Mechanism for production of phenol from benzene through an oxygen transfer process using: (a) water (b) O_2 as oxygen source [74].

Author's personal copy

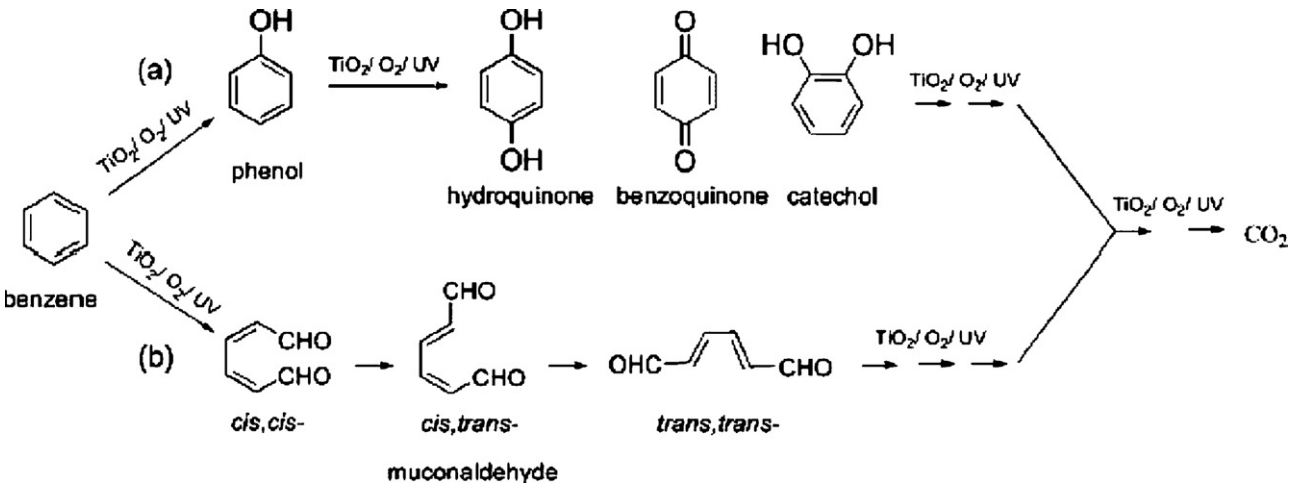

Fig. 17. Two pathways for decomposition of benzene on TiO_2 photocatalyst: (a) via phenol and (b) via muconaldehyde [75].

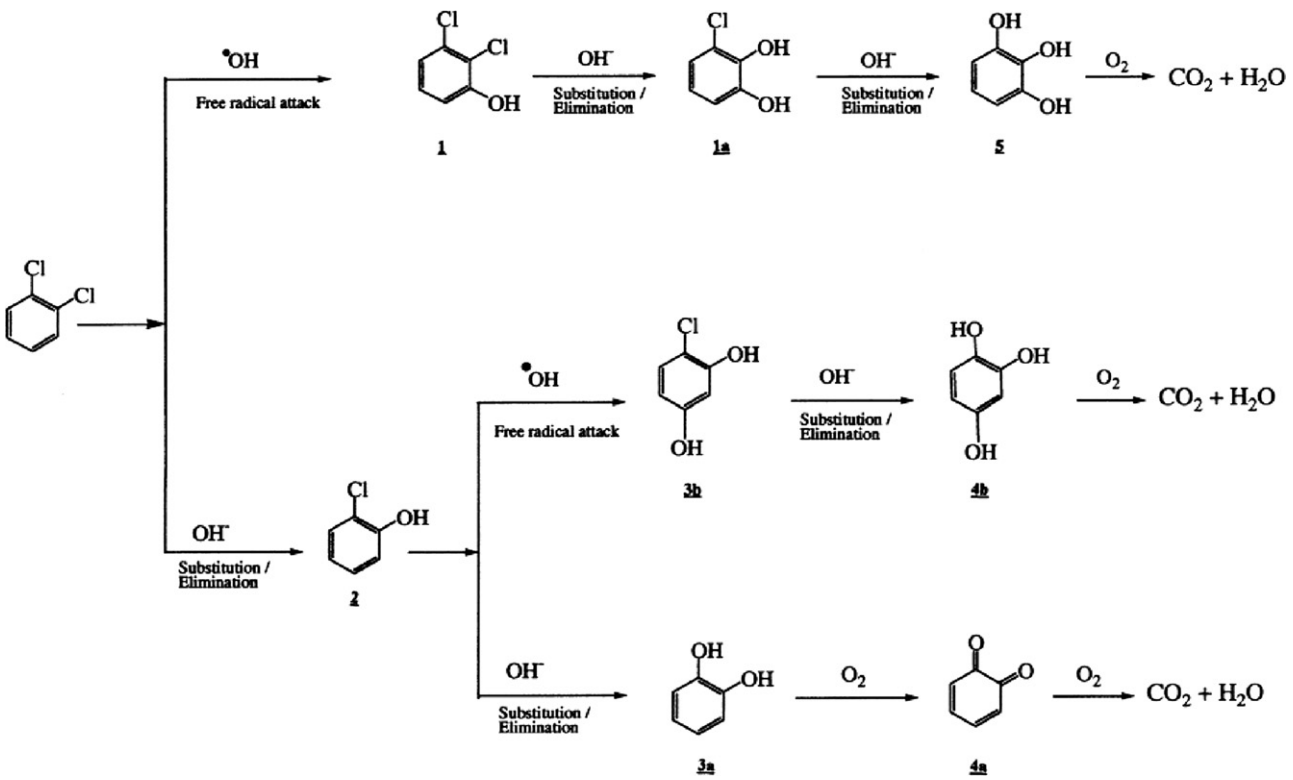

Fig. 18. Proposed dichloro-benzene photocatalytic oxidation mechanism in TiO_2 suspensions [78a].

respectively, to oxygen transfer and hole transfer processes in the initial step of benzene oxidation. Cation radicals, which are formed by the hole transfer mechanism, are the species that react with oxygen, as shown in Fig. 16. The peroxide radical formed as a result of the reaction between the benzene cation radical and an O_2 molecule can be converted to phenol through reductive processes, for which a variety of intermediates produced before conversion into CO_2 may be used as reductants. In addition to molecular oxygen, $O_2^{\bullet-}$, produced by reduction of O_2 on TiO_2 may also be used in the reaction with benzene cation radicals. The authors, moreover, demonstrated that in the presence of anatase powders, 70–90% of oxygen introduced into phenol was from water. On the contrary, when rutile powders were used, only 20–40% of the oxygen was from water. The rest was from molecular oxygen in both cases.

In a subsequent study [75] the same authors using ^{13}C isotope clarified the initial oxidation process of benzene: muconaldehyde (Fig. 17), one of the intermediate of the degradation of benzene, was not produced from phenol, indicating that the two products are produced by independent pathways. The pathway via phenol accounts for 30–40% and the pathway via muconaldehyde accounts for 60–70% of benzene consumption. Muconaldehyde is easily oxidized to carboxylic acids, which is then mineralized successively. On the contrary, it is rather difficult to oxidize phenol and phenolic compounds. As a result, CO_2 is mostly produced via the muconaldehyde pathway while benzene is oxidized.

Chloro-benzenes are for instance target compounds that have been deeply studied due to their frequent use as intermediates in the production of commodities such as herbicides, dyestuffs, and

Author's personal copy

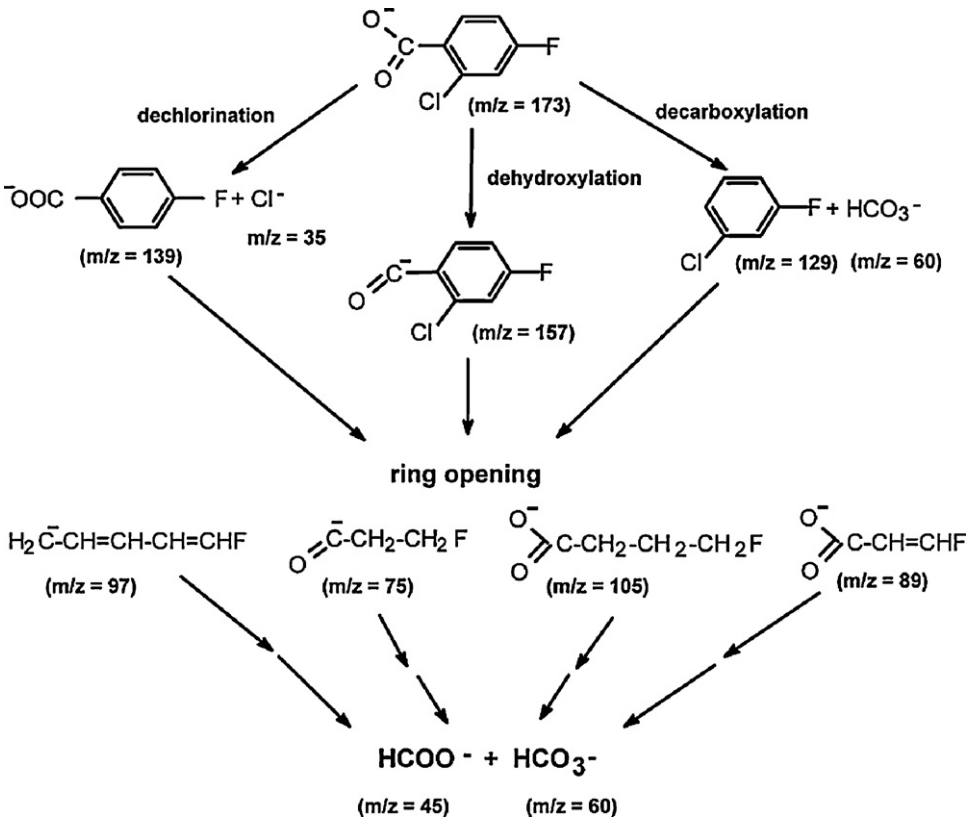

Fig. 19. Proposed 2-chloro,4-fluoro benzoic acid photocatalytic oxidation mechanism in TiO_2 suspensions [79].

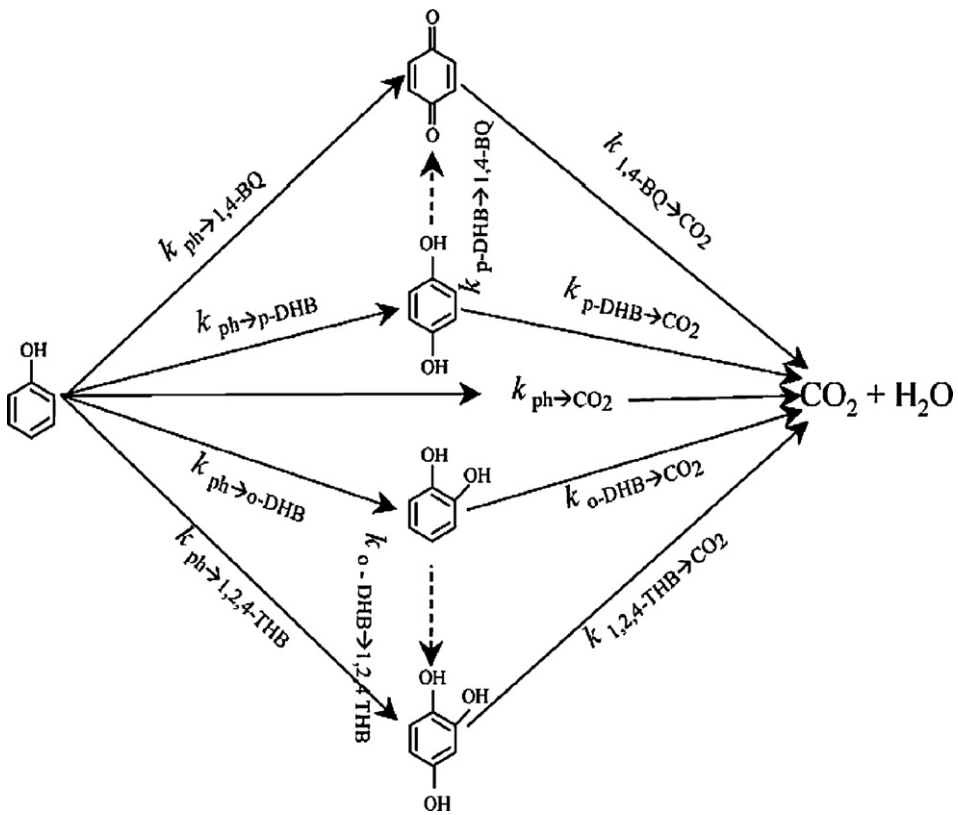

Fig. 20. Proposed phenol photocatalytic oxidation mechanism in TiO_2 suspensions [89].

Author's personal copy

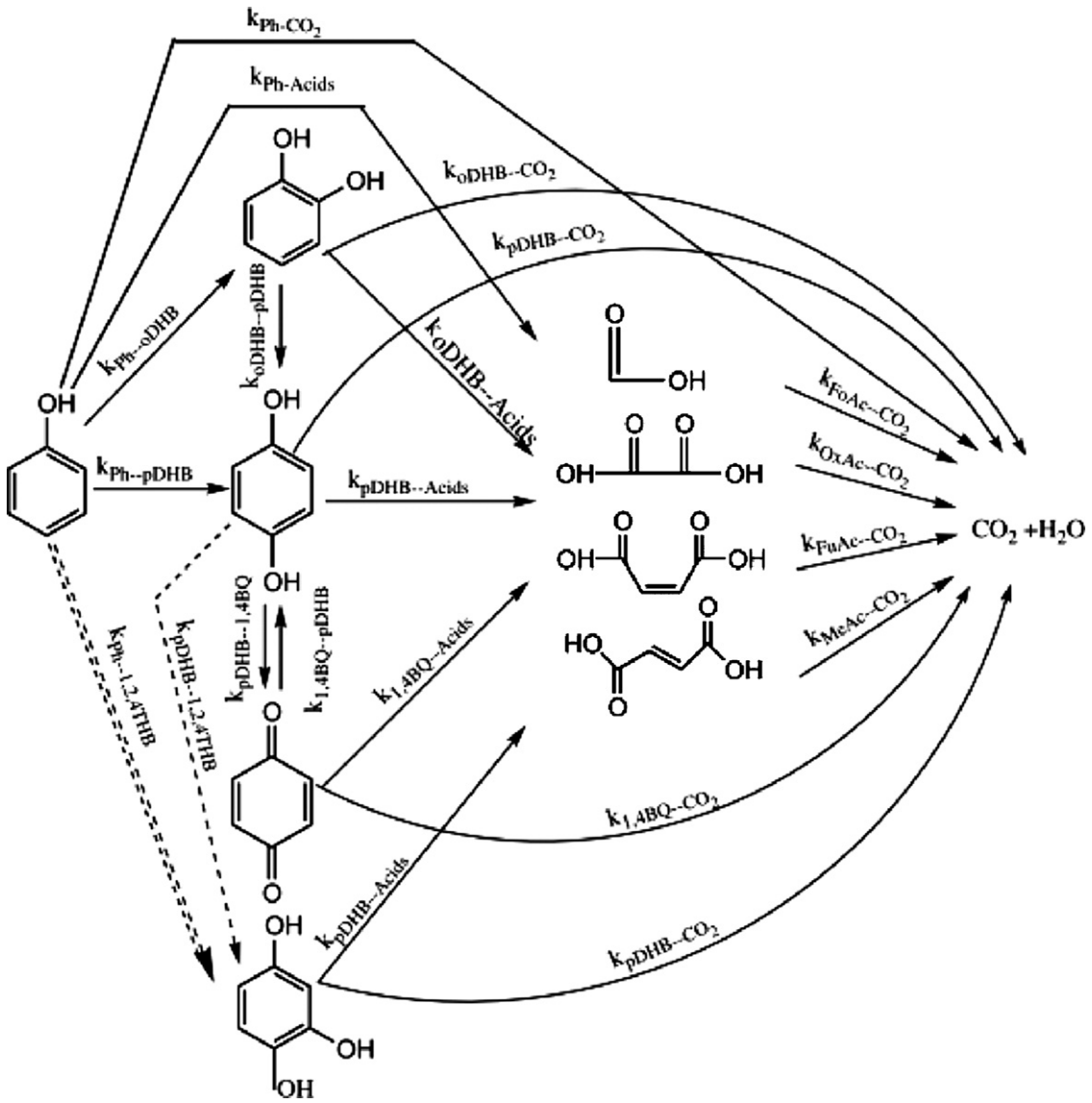

Fig. 21. Proposed phenol photocatalytic oxidation mechanism in TiO_2 suspensions [90].

rubber [78]. In particular dichlorobenzene photocatalytic oxidation has been studied in a batch slurry reactor and in a semi-batch reactor with continuous recycle with titania immobilized on inert supports [78a]. The mechanism, corroborated by HPLC and GC/MS analysis, involves hydroxyl radical that attacks the meta position of dichlorobenzene (DCB) to generate 2,3-dichlorophenol, as showed in Fig. 18. Substitution of a chloro-group by hydroxyl group generates 2-chlorophenol (2), which subsequently may lead to the formation of hydroquinone or 1,2-dihydroxybenzene (3a) and *o*-benzoquinone (4a). Further analogous substitutions on 2,3-dichlorophenol (1) will lead to 1,2,3-trihydroxybenzene (pyrogallol) (5). The ultimate oxidation products are chloride ions in solution. Moreover the formation of various organic acids was qualitatively proved and the pH of solution changes from neutral to acidic due to organic acids and CO_2.

Fluorinated aromatics can usually pollute the natural environment and condensate in living bodies. Moreover environmentally persistent compounds such as fluoride–chloride-bearing aromatics (such as cyanuric acid) present a formidable challenge in their disposal. Photocatalytic oxidation mechanisms have been deeply studied, as for instance in the case of chloro/fluoro-benzoic acid derivatives [79].

A mechanism of the partial oxidation of 2-chloro,4-fluoro benzoic acid has been proposed (Fig. 19) on the basis of the obtained mass spectral patterns. OH radicals give rise to oxidation generally attacking substrates at positions of the highest electron densities. Fig. 19 shows that the primary step can be dechlorination, decarboxylation, or dehydroxylation, whereas defluorination is hindered due to the energy of the C—F bond, that is much greater than that of C—Cl bond. Open-ring products are finally intermediates through which total oxidation occurs giving rise to formic acid and CO_2. It should be underlined that dechlorination typically appears to be somewhat faster than photodegradation through ring cleavage and evolution of carbon dioxide (photomineralization).

The phenolic compounds are used as raw material in chemical industries and agriculture productions and their presence in the air and in aqueous effluents cause environmental problems because of their high toxicity and bio-recalcitrant nature [80–86]. Phenol photocatalytic oxidation mechanisms have been deeply studied and intermediates carefully identified and analyzed [87–90]. Parallel oxidation pathways take place like for several other organics, yielding poly-hydroxylated derivatives, and namely 1,4-dihydroxybenzene, 1,2-dihydroxybenzene and 1,2,4-trihydroxybenzene (Fig. 20), along with CO_2. The first species

Author's personal copy

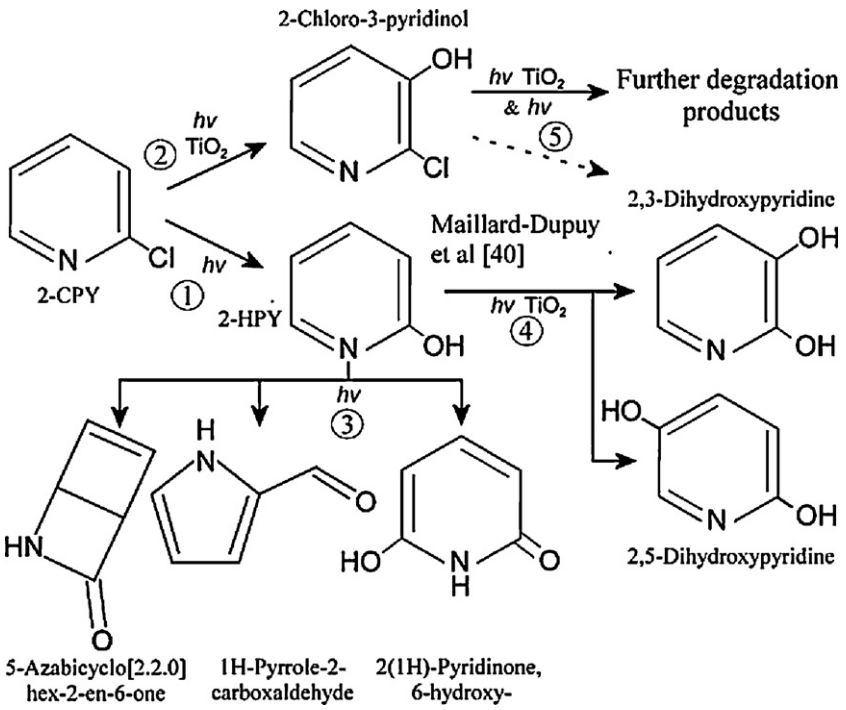

Fig. 22. Key early stage intermediate compounds and reaction pathways during the 2-CPY combined photolytic/photocatalytic degradation in TiO_2 suspensions [93].

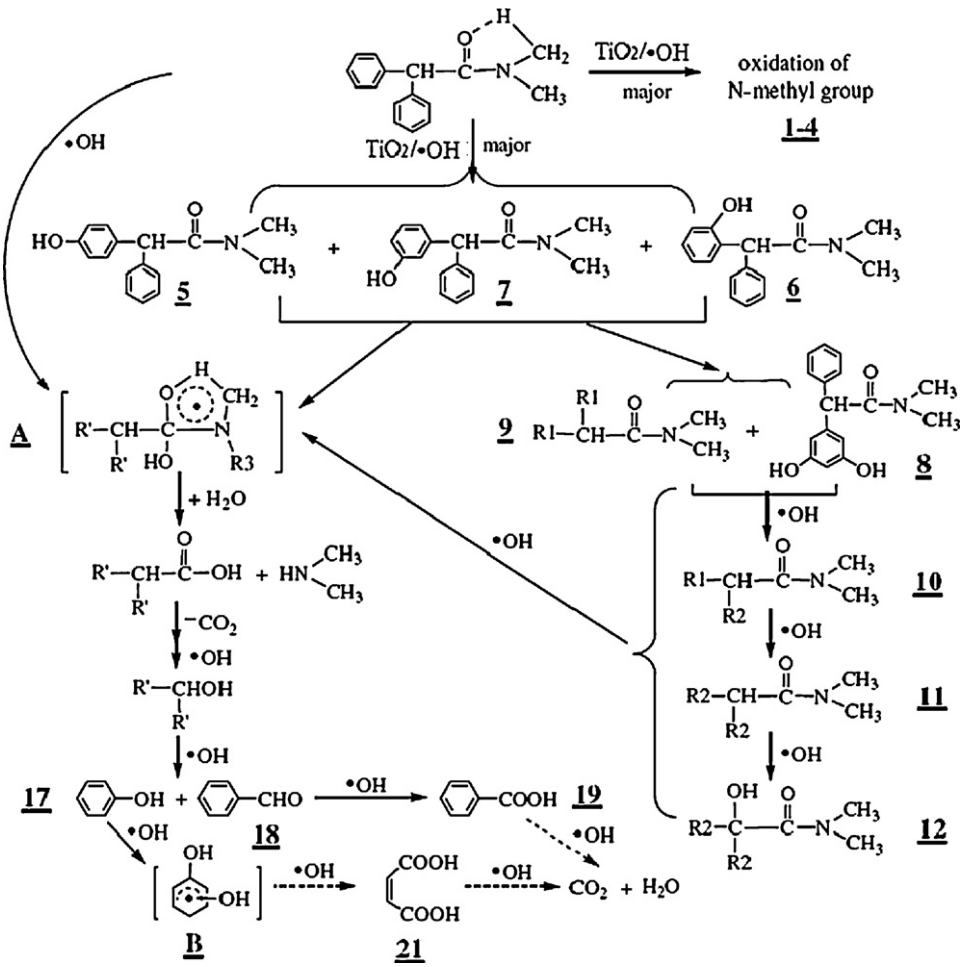

Fig. 23. Pathways of diphenamid degradation via TiO_2/UVA [94].

Author's personal copy

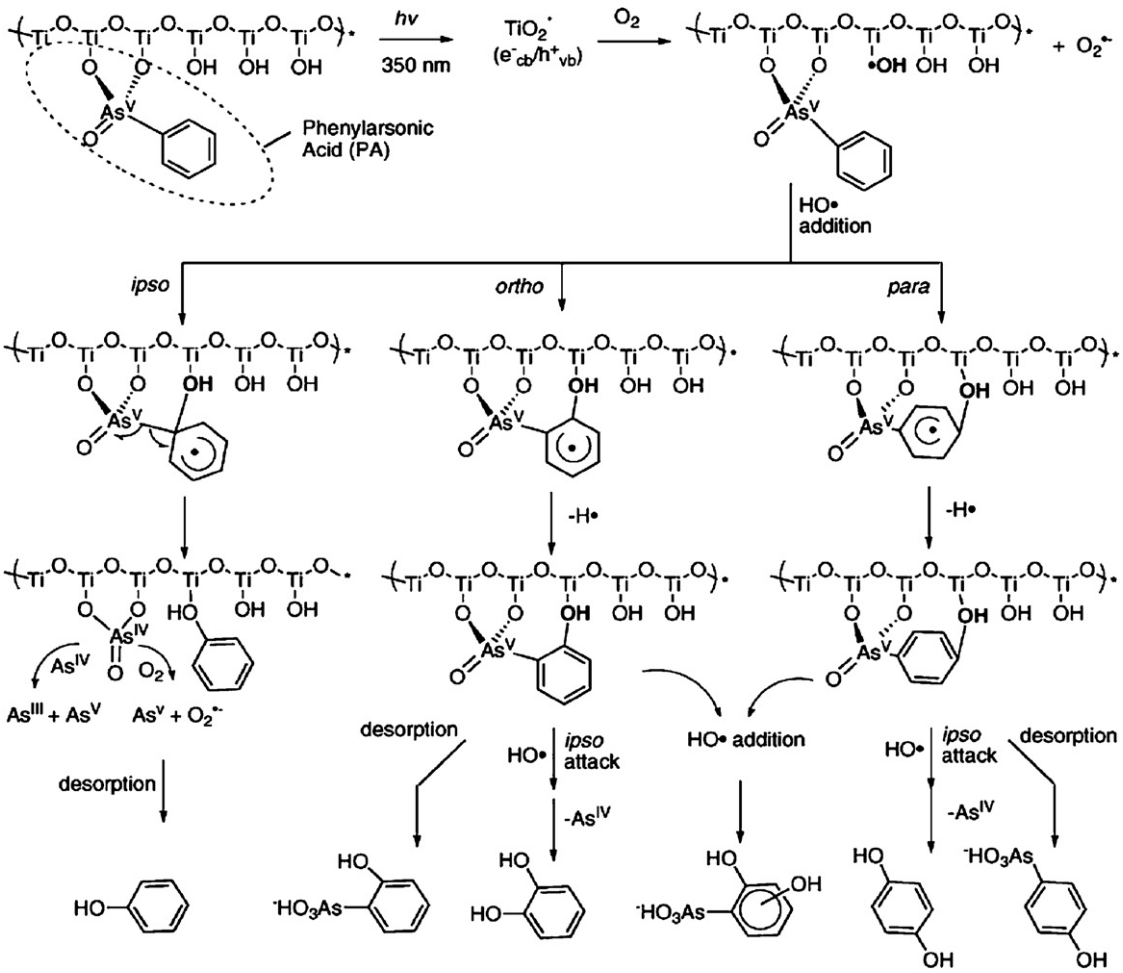

Fig. 24. Pathways of photocatalytic degradation of phenylarsonic acid [95].

participates to a ketoenolic equilibrium giving rise to benzoquinone, whereas 1,3-dihydroxybenzene has never been detected, accordingly to the general rule that one electron donor group impedes the entrance of hydroxyl radical in meta position [91].

Formation of various open-ring intermediates has also been proved (Fig. 21) and in particular fumaric acid (FuAc), maleic acid (MaAc), oxalic acid (OxAc) and formic acid (FoAc). A detailed kinetics has also been developed, based on Langmuir–Hinshelwood model, considering most of the series-parallel reactions demonstrated [90].

High phenol concentrations (>1 g/L) can yield peroxocompound formation which is not affected by the hydroxyl radical insertion process. This is due to the higher amount of chemisorbed phenol molecules, which causes that fewer photons reach the surface and lower amounts of hydroxyl are formed. Consequently, holes can generate phenol-like species, which subsequently yield phenoxy radicals. The process in this case may be driven by the interaction of these species with $^{\bullet}O_2$ and the degradation cycle is then completed on the catalyst surface [92].

Pyridine and pyridine derivatives are widely used for the production of pesticides, medicinal drugs, industrial solvents, dyes and rubber chemicals, thus they are often encountered in wastewater and must be degraded because of their dangerous effects on human health. Combined photolytic/photocatalytic degradation of 2-chloropyridine (2-CPY), 2-fluoropyridine (2-FPY) and 2-hydroxypyridine (2-HPY) has been recently studied [93].

Wavelengths higher than 290 nm have been used in order to study the pure photocatalytic degradation (TiO_2 Degussa P25 was used as catalyst), whereas irradiation at 254 nm was applied in order to study the combined degradation. In the latter case, photolytic 2-CPY removal rate was found to be unaffected by pH, whereas its photocatalytic degradation rate was found to depend on pH, probably due to substrate adsorption, which typically depends on pH. The addition of chloride ions (in large amounts) resulted in a decreased rate of degradation, while the addition of the same ion in stoichiometric amounts with respect to the reagent caused negligible effect on this rate. On one contrary the influence of fluoride ions was very impressive in improving degradation rate that was about doubled.

In the pure photocatalytic degradation of 2-CPY, a hydroxylation reaction occurs on the position 3 and the chloride position is left intact, unlike in the direct photolysis (Fig. 22).

Photocatalytic degradation of 2-CFY gave rise to several species, including someone deriving from coupling reactions, such as 2,2′-5-fluoro-bipyridine and 2,2′-5-fluoro-4-hydroxy-bipyridine, and others deriving from ring opening, such as N-formyl-3-carbamoylpropenal. 2-CPY conversely did not give rise to coupling species.

Herbicide diphenamid (DPA) photodegradation has been studied both in homogeneous and heterogeneous conditions, under UVC (254 nm) in the former case and UVA (350 nm, coupled to TiO_2 films) in the latter case [94]. Direct photolysis with UVC showed that DPA was totally degraded after 360 min at pH 3.5, 7.2 and 9.6, whereas the corresponding organic carbon was only reduced by 11%, 8% and 9%, respectively. This behavior can be ascribed to the poor selectivity of photocatalytic processes that are

Author's personal copy

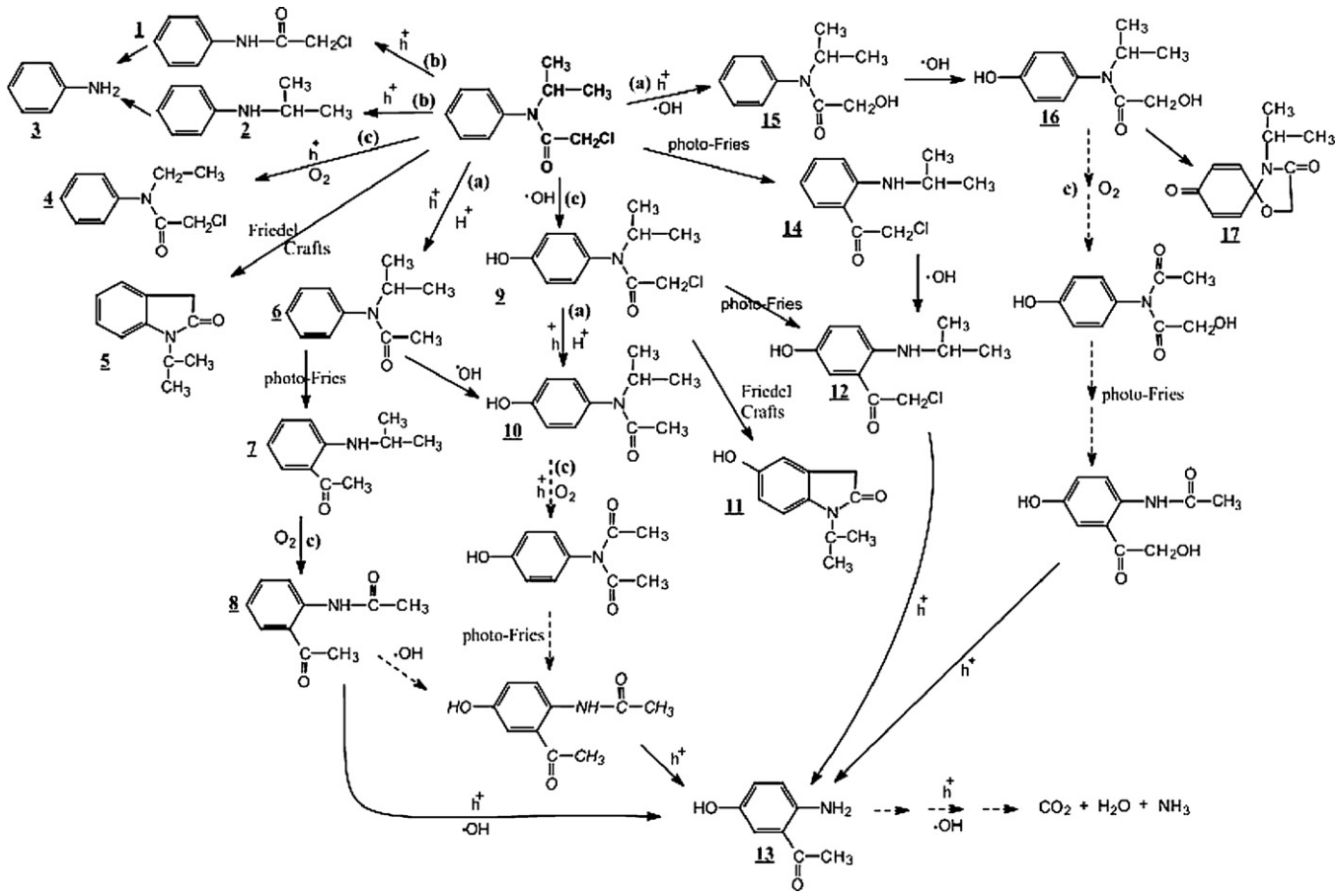

Fig. 25. Proposed pathways of photocatalytic degradation of propachlor [96].

able to carry out mineralization of several species differently from photolysis.

LC–MS and ^{1}H NMR analyses were used to detect the produced intermediates: authors identified three principal groups of intermediate products in both homogeneous and heterogeneous degradation processes: (i) products from the reactions relevant to only the N-methyl oxidation or replacement; (ii) products from the reactions of the hydroxylation of the aromatic ring; and (iii) products from the N-demethylation, oxidation and ring opening. In particular the reaction mechanism proposed for photocatalytic degradation is represented in Fig. 23: in the first step the hydroxyl radical enters aromatic ring and it is worth noting that isomer 5 showed the highest concentration level, followed by isomers 6 and 7. These results indicate that the monohydroxylation of aromatic ring with corresponding H abstraction by hydroxyl radical attack took place regioselectively on the aromatic ring. Further attack of OH radical to the aromatic ring also occurred but as a minor route. Conversely breakage of aromatic ring was favored to yield for instance maleic acid (compound 21). The ring opening was possibly due to the formation of a hydroxycyclohexadienyl radical in photocatalytic process (e.g. radical B). Moreover, both oxidation of N-methyl groups and N-demethylation on the urea moiety of DPA were also proposed (mechanism not shown).

Organoarsenic compounds are often found into the environment because they are produced by agricultural applications. Phenylated arsenic compounds such as 4-hydroxy-3-nitrophenylarsenic acid (roxarsone), 4-aminophenylarsenic acid (p-arsanilic acid) and phenylarsonic acid are commonly utilized in the broiler poultry industry as feed additives to control cecal coccidiosis. Phenylarsonic acid, in particular, has been photocatalytically degraded and the mechanism of its oxidation has been deeply investigated [95].

Photoreactions in the presence and absence of TiO_2 Degussa P25 were performed and it was found that monohydroxylated and dihydroxylated phenylarsonic acids are intermediate products present at relatively low concentrations (<10%) during TiO_2 photocatalysis, whereas under homogeneous conditions computational and product studies suggest that •OH radical preferentially adds to the ortho- and para-positions of PA, yielding 2- and 4-hydroxyl adducts as the major initial products. Conversely phenol, catechol and hydroquinone are major degradation products in heterogeneous conditions. As showed in Fig. 24, the strong adsorption of phenylarsonic acid and hydroxylated phenylarsonic acid to the TiO_2 surface, where hydroxyl radicals are localized, probably enhanced the dihydroxylation. The absence of meta- isomer was attributed to the electronic directing effect of the arsenate group in the parent compound.

Propachlor (2-chloro-*N*-isopropylacetanilide) is one of the most used herbicide in European countries and its degradation under irradiation was studied in the presence of TiO_2 Degussa P25, particularly focusing on reaction mechanism [96]. GC–MS analysis has supported the pathway represented in Fig. 25. The reactions may involve either addition of hydroxyl radicals or direct hole transfer to the organic substrate by three possible routes.

Dechlorination – route (a) of Fig. 25 – can occur through positive holes or solvated electrons, to form the hydroxyl or aliphatic derivatives. The hypothesized route (b) consists of scission of the amide bond or the N—C bond via nitrogen ionization by positive holes leading to the formation of compounds 1, 2, 3 and 13. In the route (c), finally, hydrogen abstraction takes place, followed either by the addition of oxygen to the alkyl radical

Author's personal copy

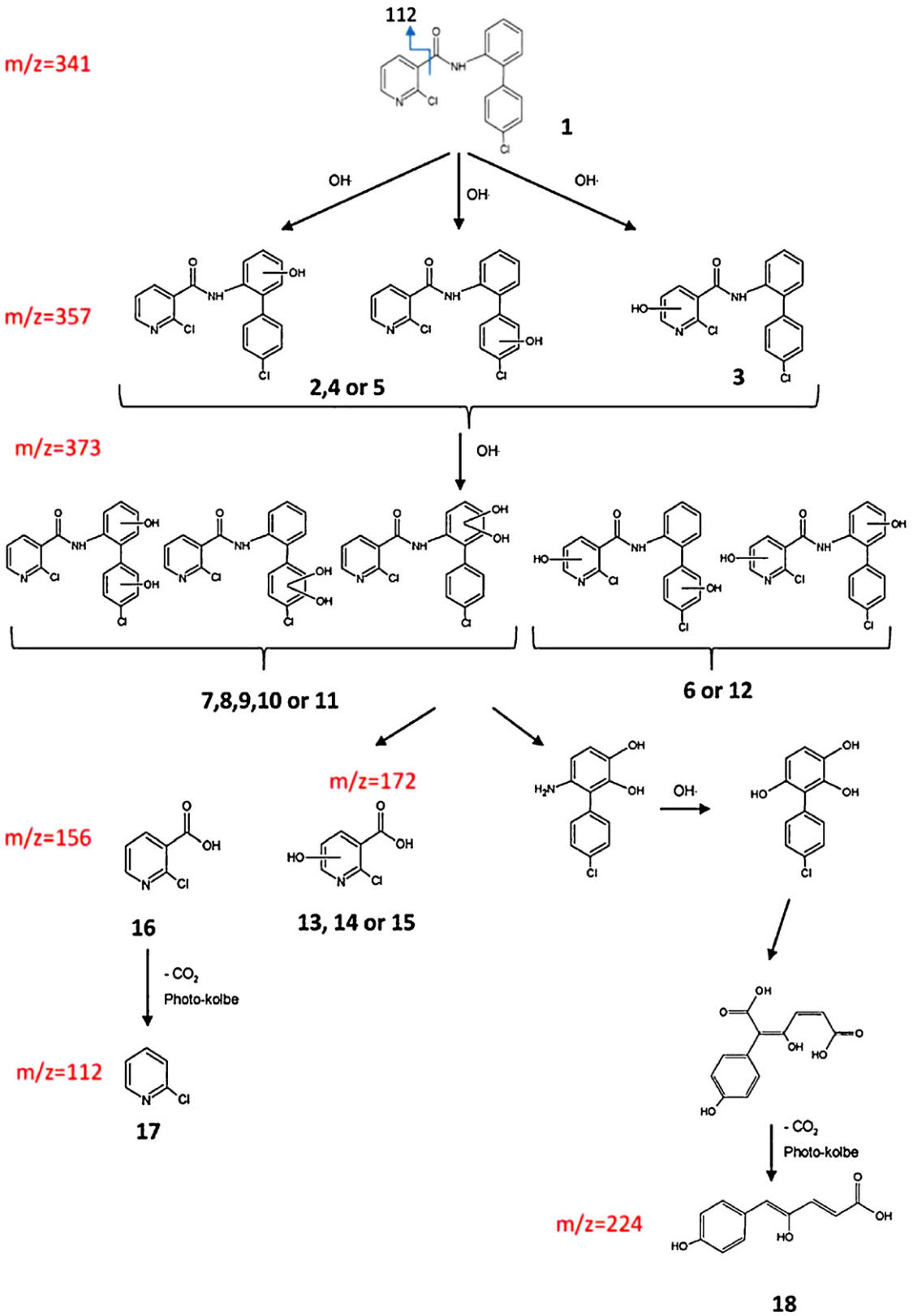

Fig. 26. Proposed pathways of photocatalytic degradation of boscalid [97].

and decomposition of the peroxyl radical formed or by hydroxylation of the ring. Products 9 and 16 were favored because hydroxyl radicals preferentially attack the aromatic moiety due to its electrophilic character. Species 5 and 11 were probably formed from the produced organic cation through the attack by the positive holes to the position 2 of the aromatic ring followed by the Friedel–Crafts reaction. Lastly, the compounds 7, 12, and 14 derived probably by the breakage of the amide bond and the attack of the chloroacetyl group in the positions ortho, meta or para. Alkylation was found to occur preferentially in ortho

Author's personal copy

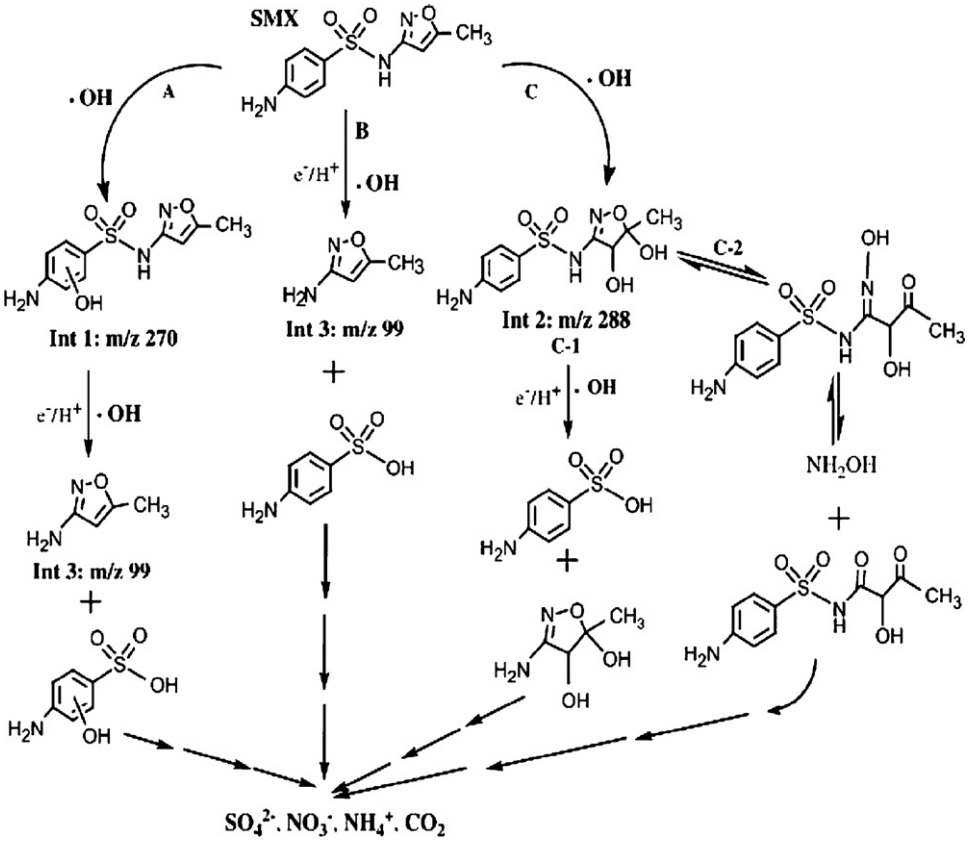

Fig. 27. Proposed pathways of photocatalytic degradation of sulfamethoxazole [98].

position, accordingly to the ortho/para orienting effect given by amino group.

Among fungicides applied to preserve grapes from disease, boscalid [2-chloro-N(4′-chloro-biphenyl-2-yl)-nicotinamide] is a completely new active ingredient belonging to the anilid group of fungicides; this compound follows a completely novel mode of action for the prevention and treatment of the grey mold (*Botrytis cinerea*) in fruit plants and vines. Its treatment in waters is important because this species is a persistent pollutant [97]. Photocatalytic transformation of boscalid has been studied in the presence of TiO_2 and UV light, with a particular care to reaction mechanisms. HPLC–MS/MS analysis has proven the presence of various intermediates suggesting the pathway reported in Fig. 26.

Boscalid was first attacked by OH radicals both in aromatic ring and in pyridine one, yielding four mono-hydroxylated products (2–5). Product 2 was the major hydroxylation intermediate whereas products 3–5 are much less important and are formed at very low concentrations, indicating a regioselective attack for the hydroxyl radicals due to the highest electron density of the benzene carbon sites. Moreover hydroxyl radicals attack took place mainly on the carbon in ortho position with respect to chloride atom probably due to its higher nucleophility. Further hydroxylation of the first intermediates (2–5) lead to seven dihydroxylated products (6–12). Product 11 was the most abundant among those, indicating that the OH radicals attack occurs mainly in benzene rings and hydroxylation of pyridine moiety represents only a minor pathway. The ultimate intermediates were formed from the scission of the amide bond (N—C bond) leading to the formation of compounds 13–18. As showed in Fig. 26, products 13–15 resulted from the breakage of the amine bond in molecules with the pyridine moiety hydroxylated (3, 6 and 12) and the product 16 from the dihydroxylated products only in benzene rings (7–11). The product 16 is the most abundant. Moreover, the products dihydroxylated with the two hydroxyl groups in neighbor carbon sites could be transformed in product 18 by the opening of the aromatic ring observed throughout the photocatalysis process and a final step of decarboxylation via photo-Kolbe reaction. Finally mineralization is the last step of the oxidation process as often in photocatalytic degradations.

The presence of pharmaceutically active compounds in aquatic environments [98,99] is raising public health concerns and, as a result, there is a growing interest in the development of innovative technologies to efficiently transform these compounds to non-toxic and pharmaceutically inactive byproducts. Among pharmaceutics the photocatalytic degradation mechanism of sulfamethoxazole (SMX) has been deeply studied in aqueous suspensions of nanostructured TiO_2 [98]. SMX was mineralized by TiO_2 irradiated with ultraviolet-A light. Surprisingly reaction rates were not sensitive to changes in sulfonamide structure; indeed substituting SMX with analogues species such as sulfisoxazole or sulfathiazole did not yield significant changes in rates. Fig. 27 shows the hypothesized mechanism initiated by OH attack on either the aromatic or heterocyclic rings or the sulfonamide bond. Three pathways (A, B, and C) were proposed based upon identification carried out by LC/MS/MS. In pathway A the addition of a hydroxyl radical to the aromatic ring formed a hydroxycyclo-hexadienyl radical (not shown in Fig. 27), from which a second hydroxyl radical can abstract another hydrogen to form the non-radical hydroxy-substituted intermediate 1. Hydroxyl radical attack on the sulfonamide bond resulted in the cleavage of the S—N bond. Further abstraction of a hydrogen by the cleaved nitrogen resulted in the formation of intermediate 3 (pathways A and B), sulfanilic acid (pathways B and C) and hydroxysulfanilic acid (pathway A). Pathway C was initiated by formation of the dihydroxy-substituted intermediate 2. This can be degraded by hydroxyl radical attack on the S—N bond (pathway C-1) or alternatively rearranged to a carbonyl prior to hydroxyl radical attack on the S—N bond via a hemi-ketal equilibrium step that cleaves the

Author's personal copy

heterocyclic ring at the O—C bond and forms an oxime at the N—O position (pathway C-2). Addition of water causes the formation of a second carbonyl. The dihydroxy isoxazole intermediate depicted in pathway C-1 could also be subject to hemi-ketal rearrangement.

4. Conclusions

This review provides the reader with a general overview on heterogeneous photocatalytic oxidation mechanisms, with a special address to conversion of aliphatic and aromatic organic species. Analysis of reactions carried out in order to perform complete degradation finalized to mineralization and photocatalytic partial oxidation has been deeply discussed.

It can be said that the oxidation of a substrate proceeds by involving not only the photogenerated holes but also the OH radicals. In particular, the oxygenation of alkanes evolves via alkyl radical reactions that lead mainly to the corresponding alcohols which can be further oxidized to the corresponding aldehydes and acids or ketones. Autooxidation reactions, of course, depending on the initial substrate, cannot be excluded; these typically occur in open air or in presence of oxygen and/or UV radiation and give rise to formation of peroxides and hydroperoxides. It was also found that oxidation attack on aliphatic organic acids is possible on different points of the molecule, and several reaction routes produce the main intermediates.

Moreover, for reactions carried out in gas phase, the role of adsorbed water was emphasized. Indeed, mechanisms mediated by OH radicals formed by holes attacking adsorbed water can strongly influence the degradation rate.

As far as the aromatic compounds are concerned, generally the oxidation proceeds via hydroxyl groups insertion. For example, for dichlorobenzene the primary attack of hydroxyl radical generates its insertion in meta position followed by the substitution of chloro-groups by hydroxyl groups before the complete mineralization.

The same mechanism was hypothesized by the photocatalytic oxidation of phenolic compounds, in which poly-hydroxylated derivatives are formed before the opening of the ring and subsequent mineralization.

In herbicide diphenamid photo-oxidation results indicated that the monohydroxylation of aromatic ring with corresponding H abstraction by hydroxyl radical attack took place regioselectively on the aromatic ring. Further attack of OH radical to the aromatic ring also occurred but as a minor route. Conversely breakage of aromatic ring was favored to yield maleic acid. Finally mineralization is the last step of the oxidation process as often occurs in photocatalytic degradations.

By concluding, many works presented were carried out under mild oxidation conditions, although it should be highlighted that organic unsafe solvents were used in most investigations.

References

[1] (a) M.R. Hoffmann, S.T. Martin, W. Choi, D.W. Bahnemann, Chem. Rev. 95 (1995) 69–96;
(b) V. Augugliaro, M. Litter, L. Palmisano, J. Soria, J. Photochem. Photobiol. C: Photochem. Rev. 7 (2006) 127–144;
(c) J. Moa, Y. Zhang, Q. Xu, J.J. Lamson, R. Zhao, Atmos. Environ. 43 (2009) 2229–2246.

[2] (a) A. Maldotti, A. Molinari, R. Amadelli, Chem. Rev. 102 (2002) 3811–3836;
(b) G. Palmisano, E. García-López, G. Marcì, V. Loddo, S. Yurdakal, V. Augugliaro, L. Palmisano, Chem. Commun. 46 (2010) 7074–7089;
(c) Y. Shiraishi, T. Hirai, J. Photochem. Photobiol. C: Photochem. Rev. 9 (2008) 157–170.

[3] (a) N. Watanabe, S. Horikoshi, H. Hidaka, N. Serpone, J. Photochem. Photobiol. A: Chem. 174 (2005) 229–238;
(b) E. García-López, G. Marcì, N. Serpone, H. Hidaka, J. Phys. Chem. C 111 (2007) 18025–18032;
(c) H. Gulyas, D. Bockelmann, L. Hemmerling, D. Bahnemann, I. Sekoulov, Water Sci. Technol. 29 (1994) 129–132.

[4] M.C. Blount, J.A. Buchholz, J.L. Falconer, J. Catal. 197 (2001) 303–314.

[5] X. Ye, D. Chen, J. Gossage, K. Li, J. Photochem. Photobiol. A: Chem. 183 (2006) 35–40.

[6] M.A. Gonzalez, S.G. Howell, S.K. Sikdar, J. Catal. 183 (1999) 159–162.

[7] M.A Brusa, Y. Di Iorio, M.S. Churio, M.A. Grela, J. Mol. Catal. A: Chem. 268 (2007) 29–35.

[8] I. Izumi, W. Dunn, K.O. Wilbourn, F.F. Fan, A.J. Bard, J. Phys. Chem. 84 (1980) 3207–3210.

[9] C.E. Taylor, Top. Catal. 32 (2005) 179–184.

[10] M.A. Gondal, A. Hameed, Z.H. Yamani, A. Arfaj, Chem. Phys. Lett. 392 (2004) 372–377.

[11] S. Suzuki, T. Tsuneda, K. Hirao, J. Chem. Phys. 136 (2012) 024706.

[12] S.I. Morten, G. Nielsen, P.C.K. Vesborg, Y. Hou, B.L. Abrams, T.R. Henriksen, O. Hansen, I. Chorkendorff, Chem. Commun. 47 (2011) 2613–2615.

[13] K. Shimura, T. Yoshida, H. Yoshida, J. Phys. Chem. C 114 (2010) 11466–11474.

[14] Y. Hu, Y. Nagai, M. Matsuoka, M. Anpo, Catal. Lett. 124 (2008) 80–84.

[15] Y. Wang, X. Wang, Z. Su, Q. Guo, Q. Tang, Q. Zhang, H. Wan, Catal. Today 93-95 (2004) 155–161.

[16] (a) A. Molinari, M. Bruni, A. Maldotti, J. Adv. Oxid. Technol. 11 (2008) 143–148;
(b) A. Molinari, M. Montoncello, H. Rezala, A. Maldotti, Photochem. Photobiol. Sci. 8 (2009) 613–619.

[17] G. Marcì, E. García-López, G. Mele, L. Palmisano, G. Dyrda, R. Słota, Catal. Today 143 (2009) 203–210.

[18] A. Mylonas, A. Hiskia, E. Androulaki, D. Dimotikali, E. Papaconstantinou, Phys. Chem. Chem. Phys. 1 (1999) 437–440.

[19] M. Zhang, Q. Wang, C. Chen, L. Zhang, W. Ma, J. Zhao, Angew. Chem. Int. Ed. 48 (2009) 6081–6084.

[20] Q. Wang, M. Zhang, C. Chen, W. Ma, J. Zhao, Angew. Chem. Int. Ed. 49 (2010) 7976–7979.

[21] V. Augugliaro, H.A. Hamed El Nazer, V. Loddo, A. Mele, G. Palmisano, L. Palmisano, S. Yurdakal, Catal. Today 151 (2010) 21–28.

[22] A. Molinari, A. Maldotti, A. Bratovcic, G. Magnacca, Catal. Today, http://dx.doi.org/10.1016/j.cattod.2011.11.033, in press.

[23] V.M. Daskalaki, P. Panagiotopoulou, D.I. Kondarides, Chem. Eng. J. 170 (2011) 433–439.

[24] K. Lalitha, G. Sadanandam, V.D. Kumari, M. Subrahmanyam, B. Sreedhar, N.Y. Hebalkar, J. Phys. Chem. C 114 (2010) 22181–22189.

[25] V. Gombac, L. Sordelli, T. Montini, J.J. Delgado, A. Adamski, G. Adami, M. Cargnello, S. Bernal, P. Fornasiero, J. Phys. Chem. A 114 (2010) 3916–3925.

[26] J.M. Meichtry, N. Quicia, G. Mailhot, M.I. Litter, Appl. Catal. B: Environ. 102 (2011) 555–562.

[27] N. Quici, M.I. Litter, A.M. Braun, E. Oliveros, J. Photochem. Photobiol. A: Chem. 197 (2008) 306–312.

[28] H. Zeldes, R. Livingston, J. Am. Chem. Soc. 93 (1971) 1082–1085.

[29] N. Quici, M.E. Morgada, R.T. Gettar, M. Bolte, M.I. Litter, Appl. Catal. B: Environ. 71 (2007) 117–124.

[30] J.C. Colmenares, A. Magdziarz, A. Bielejewska, Bioresour. Technol. 102 (2011) 11254–11257.

[31] J.M. Meichtry, N. Quicia, G. Mailhot, M.I. Litter, Appl. Catal. B: Environ. 102 (2011) 454–463.

[32] W. Irawaty, D. Friedmann, J. Scott, R. Amal, J. Mol. Catal. A: Chem. 335 (2011) 151–157.

[33] A. Danion, J. Disdier, C. Guillard, N. Jaffrezic-Renault, J. Photochem. Photobiol. A: Chem. 190 (2007) 135–140.

[34] Y. Guo, C. Hu, S. Jiang, C. Guo, Y. Yang, E. Wang, Appl. Catal. B: Environ. 36 (2002) 9–17.

[35] M.I. Franch, J.A. Ayllón, J. Peral, X. Domènech, Catal. Today 76 (2002) 221–233.

[36] I. Dolamic, T. Bürgi, J. Phys. Chem. B 110 (2006) 14898–14904.

[37] A. Jarandehei, M.K. Golpayegani, A. De Visscher, Appl. Catal. B: Environ. 84 (2008) 65–74.

[38] S. Suárez, N. Arconada, Y. Castro, J.M. Coronado, R. Portela, A. Duránb, B. Sánchez, Appl. Catal. B: Environ. 108–109 (2011) 14–21.

[39] V. Puddu, H. Choi, D.D. Dionysiou, G. Li Puma, Appl. Catal. B: Environ. 94 (2010) 211–218.

[40] G. Li Puma, I. Salvadó-Estivill, T.N. Obee, S.O. Hay, Sep. Purif. Technol. 67 (2009) 226–232.

[41] (a) M. Hegedus, A. Dombi, Appl. Catal. A-Gen. 271 (2004) 177–184;
(b) S.K. Joung, T. Amemiya, M. Murabayashi, K. Itoh, Chem. Eur. J. 12 (2006) 5526–5534;
(c) P.B. Amama, K. Itoh, M. Murabayashi, J. Mol. Catal. A: Chem. 217 (2004) 109–115;
(d) S. Rodrigues, K.T. Ranjit, S. Uma, I.N. Martyanov, K.J. Klabunde, J. Catal. 230 (2005) 158–165.

[42] A. Maldotti, A. Molinari, R. Amadelli, Chem. Rev. 102 (2002) 3811–3836.

[43] C. Murata, H. Yoshida, J. Kumagai, T. Hattori, J. Phys. Chem. 107 (2003) 4364–4373.

[44] H. Yoshida, Curr. Opin. Solid State Mater. Sci. 7 (2003) 435–442.

[45] H. Yoshida, M.G. Chaskar, Y. Kato, T. Hattori, J. Photochem. Photobiol. A: Chem. 160 (2003) 47–53.

[46] P. Calza, C. Massolino, E. Pelizzetti, J. Photochem. Photobiol. A: Chem. 199 (2008) 42–49.

[47] P. Oance, T. Oncescu, J. Photochem. Photobiol. A: Chem. 199 (2008) 8–13.

[48] N. Guettaï, A. Assabbane, H.A. Amar, Fresenius Environ. Bull. 17 (2008) 347–356.

[49] E. Evgenidou, K. Fytianos, I. Poulios, J. Photochem. Photobiol. A: Chem. 175 (2005) 29–38.

[50] W. Ren-Jang, C. Chiing-Chang, C. Ming-Hung, L. Chung-Shin, J. Hazard. Mater. 15 (2009) 945–953.

Author's personal copy

[51] P. Pichat, Water Sci. Technol. 35 (1997) 73–78.
[52] S. Higashimoto, N. Kitao, N. Yohida, T. Sakura, M. Azuma, H. Ohue, Y. Sakata, J. Catal. 266 (2009) 279–285.
[53] C. Minero, G. Mariella, V. Maurino, E. Pelizzetti, Langmuir 16 (2000) 2632–2641.
[54] S. Kim, W. Choi, J. Phys. Chem. B 109 (2005) 5143–5149.
[55] G. Palmisano, S. Yurdakal, V. Augugliaro, V. Loddo, L. Palmisano, Adv. Synth. Catal. 349 (2007) 964–970.
[56] S. Yurdakal, G. Palmisano, V. Loddo, V. Augugliaro, L. Palmisano, J. Am. Chem. Soc. 130 (2008) 1568–1569.
[57] M. Addamo, V. Augugliaro, M. Bellardita, A. Di Paola, V. Loddo, G. Palmisano, L. Palmisano, S. Yurdakal, Catal. Lett. 126 (2008) 58–62.
[58] V. Augugliaro, T. Caronna, V. Loddo, G. Marcì, G. Palmisano, L. Palmisano, S. Yurdakal, Chem. Eur. J. 14 (2008) 4640–4646.
[59] S. Yurdakal, G. Palmisano, V. Loddo, O. Alagöz, V. Augugliaro, L. Palmisano, Green Chem. 11 (2009) 510–516.
[60] S. Farhadi, M. Zaidi, Appl. Catal. A-Gen. 354 (2009) 119–126.
[61] M.A. Rauf, M.A. Meetani, S. Hisaindee, Desalination 276 (2011) 13–27.
[62] S.Y. Lu, D. Wu, Q.L. Wang, J. Yan, A.G. Buekens, K.F. Cen, Chemosphere 82 (2011) 1215–1224.
[63] L. Elsellami, S. Pigeot-Rémy, F. Dappozze, F. Vocanson, A. Houas, C. Guillard, Environ. Technol. 31 (2010) 1417–1422.
[64] A. Hakki, R. Dillert, D. Bahnemann, Catal. Today 144 (2009) 154–159.
[65] L.M. Canle, J.A. Santaballa, E. Vulliet, J. Photochem. Photobiol. A: Chem. 175 (2005) 192–200.
[66] T. Tachikawa, A. Yoshida, S. Tojo, A. Sugimoto, M. Fujitsuka, T. Majima, Chem. Eur. J. 10 (2004) 5345–5353.
[67] M. Stylidi, D.I. Kondarides, X.E. Verykios, Int. J. Photoenergy 5 (2003) 59–67.
[68] Y.Li, J. Niu, L. Yin, W. Wang, Y. Bao, J. Chen, Y. Duan, J. Environ. Sci. 11 (2011) 1911–1918.
[69] G. Marcì, A. Di Paola, E. García-López, L. Palmisano, Catal. Today 129 (2007) 16–21.
[70] Y.C. Chung, C.Y. Chen, Water Air Soil Pollut. 200 (2009) 191–198.
[71] B.L. Yuan, X.Z. Li, N. Graham, Chemosphere 72 (2008) 197–204.
[72] C.S Lua, C.C. Chen, F.D. Mai, Y.C Wu, J. Photochem. Photobiol. A: Chem. 187 (2007) 167–176.
[73] D. Robert, B. Dongui, J.V. Weber, J. Photochem. Photobiol. A: Chem. 156 (2003) 195–200.
[74] T.D. Bui, A. Kimura, S. Ikeda, M. Matsumura, J. Am. Chem. Soc. 132 (2010) 8453–8458.
[75] T.D. Bui, A. Kimura, S. Higashida, S. Ikeda, M. Matsumura, Appl. Catal. B: Environ. 107 (2011) 119–127.
[76] Y. Ide, N. Nakamura, H. Hattori, R. Ogino, M. Ogawa, M. Sadakane, T. Sano, Chem. Commun. 47 (2011) 11531–11533.
[77] R. Molinari, T. Poerio, Asia-Pac. J. Chem. Eng. 5 (2010) 191–206.
[78] (a) H. Fei Lin, R. Ravikrishna, K.T. Valsaraj, Sep. Purif. Technol. 28 (2002) 87–102; (b) W.Z. Tang, C.P. Huang, Water Res. 29 (1995) 745–756.
[79] H. Hidaka, H. Honjou, T. Koike, Y. Mitsutsuka, T. Oyama, N. Serpone, J. Photochem. Photobiol. A: Chem. 197 (2008) 115–123.
[80] L. Lagunas-Allué, M.T. Martínez-Soria, J. Sanz-Asensio, A. Salvador, C. Ferronato, J.M. Chovelon, Appl. Catal. B: Environ. 115–116 (2012) 285–293.
[81] Y. Cao, L. Yi, L. Huang, Y. Hou, Y. Lu, Environ. Sci. Technol. 40 (2006) 3373–3377.
[82] A. Topalov, D. Molnár-Gábor, M. Kosanić, B. Abramović, Water Res. 34 (2000) 1473–1478.
[83] A. Topalov, D. Molnár-Gábor, J. Csanádi, Water Res. 33 (1999) 1371–1376.
[84] A. Amine-Khodja, A. Boulkamh, C. Richard, Appl. Catal. B: Environ. 59 (2005) 147–154.
[85] R.J. Wu, C.C. Chen, C.S. Lu, P.Y. Hsu, M.H. Chen, Desalination 250 (2010) 869–875.
[86] L. Muszkat, L. Feigelson, L. Bir, K.A. Muszkat, Pest Manag. Sci. 58 (2002) 1143–1148.
[87] K. Okamoto, Y. Yamamoto, H. Tanaka, M. Tanaka, A. Itaya, Bull. Chem. Soc. Jpn. 58 (1985) 2015–2022.
[88] V. Augugliaro, L. Palmisano, A. Sclafani, C. Mineo, E. Pelizzetti, Toxicol. Environ. Chem. 16 (1988) 89–109.
[89] M. Salaices, B. Serrano, H.I. de Lasa, Chem. Eng. Sci. 59 (2004) 3–15.
[90] A. Ortiz-Gomez, B. Serrano-Rosales, H. de Lasa, Chem. Eng. Sci. 63 (2008) 520–557.
[91] G. Palmisano, V. Loddo, V. Augugliaro, L. Palmisano, S. Yurdakal, AIChE J. 53 (2007) 961–968.
[92] O. Carp, C.L. Huisman, A. Reller, Prog. Solid State Chem. 32 (2004) 33–177.
[93] D.R. Stapleton, I.K. Konstantinou, D. Mantzavinos, D. Hela, M. Papadaki, Appl. Catal. B: Environ. 95 (2010) 100–109.
[94] H. Liang, X. Li, Y. Yang, K. Sze, Chemosphere 80 (2010) 366–374.
[95] S. Zheng, Y. Cai, K.E. O'Shea, J. Photochem. Photobiol. A: Chem. 210 (2010) 61–68.
[96] I.K. Konstantinou, V.A. Sakkas, T.A. Albanis, Water Res. 36 (2002) 2733–2742.
[97] L.L.-Allué, M.-T. Martínez-Soria, J. Sanz-Asensio, A. Salvador, C. Ferronato, J.M. Chovelon, Appl. Catal. B: Environ. 98 (2010) 122–131.
[98] L. Hu, P.M. Flanders, P.L. Miller, T.J. Strathmann, Water Res. 41 (2007) 2612–2626.
[99] V. Maroga Mboula, V. Héquet, Y. Gru, R. Colin, Y. Andrès, J. Hazard. Mater. 209-210 (2012) 355–364.